https://doi.org/10.5194/acp-2022-412
Preprint. Discussion started: 18 July 2022

Atmospheric Chemistry and Physics Discussions

Validation of the TROPOMI/S5P Aerosol Layer Height using EARLINET lidars

Konstantinos Michailidis[1*], Maria-Elissavet Koukouli[1], Dimitris Balis[1], J. Pepijn Veefkind[2,3], Martin de Graaf[2], Lucia Mona[4], Nikolaos Papagiannopoulos[4], Gelsomina Pappalardo[4], Ioanna Tsikoudi[5], Vassilis Amiridis[5], Eleni Marinou[5], Anna Gialitaki[5], Rodanthi-Elissavet Mamouri[6,7], Argyro Nisantzi[6,7], Daniele Bortoli[8,9], Maria João Costa[8,9], Vanda Salgueiro[8,9], Alexandros Papayannis[10], Maria Mylonaki[10], Lucas Alados-Arboledas[11], Salvatore Romano[12], Maria Rita Perrone[12], Holger Baars[13]

[1]Laboratory of Atmospheric Physics, Physics Department, Aristotle University of Thessaloniki, Greece
[2]Royal Netherlands Meteorological Institute (KNMI), De Bilt, the Netherlands
[3]University of Technology Delft (TU Delft), Delft, 2628 CN, the Netherlands
[4]Consiglio Nazionale delle Ricerche – Istituto di Metodologie per l'Analisi Ambientale (CNR-IMAA), C. da S. Loja, Tito Scalo (PZ), Italy
[5]IAASARS National Observatory of Athens, Athens, Greece
[6]Department of Civil Engineering and Geomatics, Cyprus University of Technology, Limassol, Cyprus
[7]ERATOSTHENES Center of Excellence, Limassol, Cyprus
[8]Earth Remote Sensing Laboratory (EaRSLab), University of Évora, Évora, 7000-671, Portugal
[9]Institute of Earth Sciences (ITC) and Department of Physics, University of Évora, Évora, 7000-671, Portugal
[10]Laser Remote Sensing Unit, Department of Physics, National and Technical University of Athens, Zografou, 15780, Greece
[11]Andalusian Institute for Earth System Research, Department of Applied Physics, University of Granada, Granada, 18071, Spain
[12]Consorzio Nazionale Interuniversitario per le Scienze Fisiche della Materia and Università del Salento, Lecce, Italy
[13]Leibniz Institute for Tropospheric Research, Leipzig, Germany

***Correspondence: Konstantinos Michailidis (komichai@physics.auth.gr)**

Abstract

The purpose of this study is to investigate the ability of the Sentinel-5P TROPOspheric Monitoring Instrument (TROPOMI) to derive accurate geometrical features of lofted aerosol layers on a continental scale. Comparisons with ground-based correlative measurements constitute a key component in the validation of passive satellite aerosol products. For this purpose, we use ground-based observations from quality controlled lidar stations reporting to the European Aerosol Research Lidar Network (EARLINET). An optimal methodology for validation purposes has been developed and applied using the EARLINET optical profiles and TROPOMI aerosol products, aiming at the in-depth evaluation of the TROPOMI Aerosol Layer Height (ALH), product over the Mediterranean Basin for the period 2018 to 2021, over the Mediterranean Basin. Seven EARLINET stations across the Mediterranean were chosen, taking into consideration their proximity to the sea, which provided 34 coincident aerosol cases for the satellite retrievals. In the following, we present the first validation results for the TROPOMI/S5P ALH using the optimized EARLINET lidar products employing the automated validation chain designed for this purpose. The quantitative validation at pixels over the selected EARLINET stations illustrates that TROPOMI ALH is consistent with EARLINET, with a high correlation coefficient R=0.9 (R=0.59) and a mean bias of −1.02±0.96 km (−1.46±1.57 km) over ocean and ocean/land pixels respectively. Overall, it appears that aerosol layer altitudes retrieved from TROPOMI are systematically lower than altitudes from the lidar retrievals**.** This work confirms that the TROPOMI ALH product is within the required threshold

https://doi.org/10.5194/acp-2022-412
Preprint. Discussion started: 18 July 2022

Atmospheric Chemistry and Physics Discussions

accuracy and precision requirements of 1 km. Furthermore, we describe and analyse three case studies in detail, one dust and two smoke episodes, in order to illustrate the strengths and limitations of TROPOMI ALH product and demonstrate the presented validation methodology.

1 Introduction

Aerosols play a prominent role in atmospheric composition, climate and human health (IPCC, 2021). Given the broad variety of their natural and anthropogenic sources, their relatively short lifetime, and their different formation mechanisms, aerosols exhibit highly variable spatio-temporal distributions around the globe. Aerosol properties are one of the leading uncertainties in climate modeling; both natural and anthropogenic aerosols can strongly affect both air quality as well as the delicate balance in atmospheric chemistry. The knowledge of the vertical distribution on aerosols is an important key parameter to reduce uncertainties in our understanding of Earth's climate. Due to the high degree of variability of aerosols in time and space, this knowledge is required at a high spatio-temporal resolution. Accurate and reliable measurements of aerosol distributions and their properties such as the aerosol layer height, ALH, is essential for understanding the impact of aerosols on the climate system. Both active and passive remote sensing methods have been developed, from both ground-based and space-borne systems, in order to estimate the aerosol layer height. Lidar profiles from the European Aerosol Research Lidar Network, EARLINET, provide the accurate and reliable detailed vertical structure of the aerosols, and therefore can be regarded as the benchmark for validating passive ALH remote sensing (Pappalardo et al., 2014). Ground-based active remote sensing methods offer high accuracy results however their geographical coverage is spatially limited. Space-based instruments are able to fill this gap, providing products with global coverage. In order to trust and use the space-based products, their validation against known ground truth is required. In recent years, many Earth satellite sensors have developed algorithms to extract the ALH information from their UltraViolet/Visible (UV/VIS) observations: the MetOp Global Ozone Monitoring Experiment-2 (GOME-2) instruments (Hassinen et al., 2016), the Deep Space Climate Observatory (DSCOVR) mission with its Earth Polychromatic Imaging Camera (EPIC) (Xu et al., 2019), the Multi-angle Imaging Spectro Radiometer (MISR) on board the NASA Terra satellite (Nelson et al., 2013) and most recently the Sentinel-5P TROPOspheric Monitoring Instrument (Veefkind et al., 2012). Over the next years, upcoming missions such as the Geostationary Environment Monitoring Spectrometer (GEMS; Kim et al., 2019), and the Sentinel-4 and Sentinel-5 missions (Ingmann et al., 2012) are expected to continue providing quality-assured aerosol height datasets.

In this work, we focus on the validation of the S5P/TROPOMI Aerosol Layer Height product (Nanda et al., 2020), against independent ground-based lidar measurements in order to evaluate the quality of the TROPOMI retrievals. The European lidar network (EARLINET; Pappalardo et al., 2014), a network of ground-based lidar instruments, has been established to provide reference measurements of aerosol properties for validating TROPOMI retrievals, providing long-term, quality-assured and multi-wavelength aerosol vertical profiles. The

https://doi.org/10.5194/acp-2022-412
Preprint. Discussion started: 18 July 2022

Atmospheric Chemistry and Physics Discussions

geographic and temporal coverage of EARLINET stations along their quality assured measurements provides an excellent framework for the intercomparison of TROPOMI/S5P products under different atmospheric conditions and aerosol concentrations around Europe. The GOME2/MetOp aerosol height products have also been validated against the EARLINET ground-based lidars (Michailidis et al., 2021). At the time of writing this article, no studies assessing the calibration and validation of TROPOMI aerosol products with ground-based EARLINET stations have been published

The article is structured as follows: a general description of the region of interest is given in **Section 1.1. Sections 2.1** and **2.2** contain the description of the satellite and ground-based data sets used in the study. **Section 2.3** contains the detailed description of the validation strategy, the quality control and product limitations. In **Section 3** we provide the main validation results and statistics and also three case studies in order demonstrate the full potential of the presented method. Conclusions and prospects are summarized in **Section 4**.

1.1 Study Region: the Mediterranean Region

The Mediterranean Sea Basin consists of a region heavily influenced by the Sahara Desert on the South and the highly populated and industrialized European countries to the North. This region has been identified as a crossroad of air masses with many types of aerosols (Lelieveld et al., 2002; Basart et al. 2009; Amiridis et al., 2010; Soupiona et al., 2020). This relatively high aerosol load in the region can have strong effects on the regional radiative budget, climate, and ecosystems. Many studies have used satellite observations to derive aerosol properties over the Mediterranean during the last decade (e.g. Gerasopoulos et al. 2011; Mallet et al., 2013; Nabat et al., 2013; Marinou et al, 2017; Papanikolaou et al., 2020) and investigate their effect on radiation, cloud formation and climate (e.g. Georgoulias et al., 2020.)

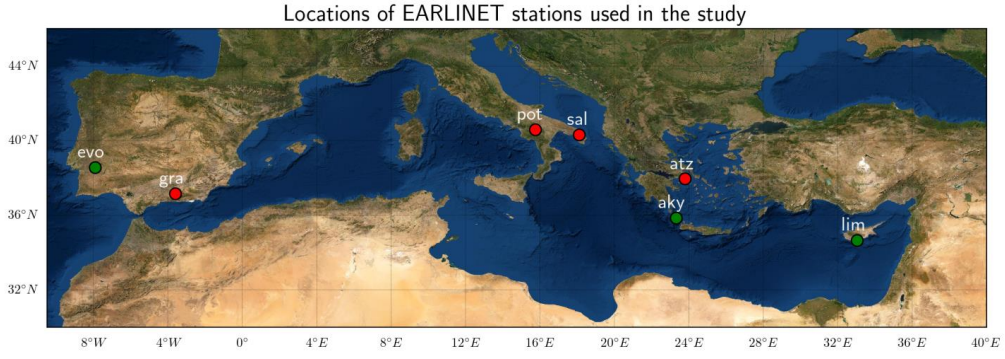

Figure 1. Location of the EARLINET lidar stations used in this study. Red circles denote multi-wavelength Raman lidars and green circles denote the stations with continuous operation capabilities (see Table 1).

Figure 1 shows the geographical distribution of the selected EARLINET stations participating in the TROPOMI-EARLINET intercomparison activity (in alphabetical order: Antikythera-PANGEA, Athens, Evora, Granada, Lecce, Limassol and Potenza). The sites are located around the Mediterranean basin and were chosen

https://doi.org/10.5194/acp-2022-412
Preprint. Discussion started: 18 July 2022

110 to represent different latitudes, longitudes and topography. **Table 1**provides the locations of the EARLINET stations along with their identification codes, surface elevation and respective references. The location of the stations across the Mediterranean basin is an ideal test environment for TROPOMI ALH features due to their proximity to the Sahara Desert and Europe, with frequently observed events of mineral dust and smoke particles. Thence, the TROPOMI aerosol products can be examined under a complete set of different atmospheric
115 conditions. Over land, the TROPOMI ALH product has decreased capabilities compared to over the sea surfaces since, over bright surfaces, the retrieval algorithm becomes increasingly sensitive to errors in the surface albedo features (Griffin et al., 2020). All participating stations operate high-performance multi-wavelength lidar systems. Three of the contributing stations (Antikythera-PANGEA, Evora and Limassol since 10.2021) are also part of the PollyNET sub-network (http://polly.tropos.de, last access: 01 May 2022), operating 24/7 portable,
120 remote-controlled multiwavelength-polarization Raman lidar systems (PollyXT; Baars et al., 2016; Engelmann et al., 2016).

Table 1. Details on the locations and main reference document for the EARLINET lidar stations used in this work.

Station	Code	Country	Longitude, latitude, elevation	Main References
Antikythera-PANGEA	AKY	Greece	23.31ºE, 35.86ºN, 193m	Kampouri et al. (2021)
Athens	ATZ	Greece	23.78ºE, 37.96ºN, 212m	Pappayannis et al. (2020)
Évora	EVO	Portugal	7.91ºW, 38.56ºN, 293m	Salgueiro et al. (2021)
Granada	GRA	Spain	3.60ºW, 37.16ºN, 680m	Guerrero-Rascado et al. (2009)
Lecce	SAL	Italy	18.10ºE, 40.33ºN, 30m	Perrone et al. (2019)
Limassol[1]	LIM	Cyprus	33.04ºE, 34.67ºN, 10m	Nisantzi et al. (2015)
Limassol[2]	CYC	Cyprus	33.03ºE, 34.67ºN, 10m	Mamouri et al. (2021)
Potenza	POT	Italy	15.72ºE, 40.60ºN, 760m	Madonna et al. (2011)

[1]Cyprus University of Technology (CUT)
125 [2]Leibniz Institute for Tropospheric Research, Leipzig and ERATOSTHENES Centre of Excellence (after Oct 2020)

2 Data and methodology

2.1 The EARLINET products

130 The lidar technique is the most predominant tool for aerosol profiling and has largely contributed to our knowledge of the vertical distribution of the aerosol optical properties (e.g., Balis et al., 2004; Papayannis et al., 2008; Mona et al., 2012; Granados-Muñoz et al., 2016; Ortiz-Amezcua et al. 2017). The European Aerosol Research Lidar Network (EARLINET; https://www.earlinet.org/, Pappalardo et al., 2014), established in 2000, provides an excellent opportunity to provide a large collection of quality-assured ground-based data of the

https://doi.org/10.5194/acp-2022-412
Preprint. Discussion started: 18 July 2022

vertical distribution of the aerosol optical and geometrical properties over Europe. Currently, the network includes 32 active lidar stations distributed over Europe, providing information of aerosol vertical distributions on a continental scale. The large majority of the involved stations is based on multi-wavelength Raman lidar systems, that combine detection channels at both elastic and Raman-shifted signals,and are equipped with depolarization channels EARLINET measurements follow absolute accuracy standards to achieve the desired confidence in product calculations. To this end, the lidar measurements are processed by the Single Calculus Chain (SCC) (D'Amico et al., 2015, 2016), the standardized tool that allows a centralized process of the lidar data acquired at each station within EARLINET. Furthermore, in order to ensure qualitative and consistent data processing within the EARLINET network, algorithm intercomparison campaigns have been organized (e.g. Amodeo et al., 2018). The main information stored in the files of the EARLINET database is the vertical distribution of aerosol backscatter and aerosol extinction coefficients together with their errors, mainly at one or more out of the following wavelengths: 355 nm, 532 nm and 1064 nm. The database also includes volume and particle depolarization ratio profiles at 532 nm (some stations also at 355 nm). During daytime, the Klett-Fernald (KF) method (Fernald, 1984; Klett, 1981) is applied using the elastic signals due to the low signal-to-noise ratio at the Raman channels. On the other, during nighttime, extinction and backscatter coefficient profiles at 355 and 532 nm can be determined independently using the Raman method (Ansmann et al., 1992). In this study, the lidar data were analyzed using the KF method whenever the weather conditions were adequate and the signal quality was sufficient for deriving high-quality backscatter vertical profiles. The EARLINET data have been used extensively for satellite aerosol products validation in recent years, such as for the Cloud-Aerosol Lidar and Infrared Pathfinder Satellite Observations (CALIPSO) (Winker et al., 2009), which is the first satellite focused on monitoring vertically resolved aerosol and cloud optical products (Papagiannopoulos et al., 2016). Furthermore, the evaluation of aerosol optical products from the Cloud-Aerosol Transport System (CATS) on board the International Space Station (ISS) was also performed based on the EARLINET database (Proestakis et al., 2019). Recently, the co-polar particle backscatter coefficient product measured by the Atmospheric LAser Doppler INstrument (ALADIN) onboard Aeolus, was evaluated in the Iberian Peninsula using EARLINET data (Abril-Gago et al., 2021).

With respect to the aerosol layer height reported by UV-VIS satellite sensors, Michailidis et al., (2021) have successfully validated the GOME2/MetOp Absorbing aerosol height (AAH) products using aerosol profiles reported by the EARLINET community. The intercomparison showed that the GOME-2 AAH measurements provide a good estimation of the aerosol layer altitudes sensed by the EARLINET ground-based lidars with a mean bias of approximately −0.2±1.7 km. While the TROPOMI ALH has more observations of dust and smoke outflows over the water surfaces, the GOME-2 AAH has improved availability over desert regions and remote oceans as its retrieval has no constraint on surface albedo and cloud fraction. A recent validation study of TROPOMI operational ALH retrievals against the CALIOP data by Nanda et al. (2020) indicated that operational algorithm retrieves lower ALH compared to CALIOP, by ~ 2 km over land and ~ 0.5 km over ocean. A similar comparison for the North American fires during the 2018 season (Griffin et al., 2020) indicates that

https://doi.org/10.5194/acp-2022-412
Preprint. Discussion started: 18 July 2022

Atmospheric Chemistry and Physics Discussions

this absolute bias also strongly depends on the smoke plume thickness, which controls the relative contribution of the satellite instrument signal from the surface. They reported that a −2.1 km bias of ALH is found for thin smoke plumes which is reduced to only −0.7 km on average for plumes thicker than 1.5 km. The remaining bias can be attributed to different studied plume characteristics (i.e. plume top vs plume centroid).

2.2 The TROPOMI/S5P Aerosol Layer Height

The TROPOspheric Monitoring Instrument (TROPOMI; Veefkind et al., 2012) is a space-borne, nadir-viewing, imaging spectrometer operating in a non-scanning push broom configuration covering wavelength bands between the ultraviolet and the shortwave infrared. Sentinel-5P is a near-polar sun-synchronous orbit satellite flying at an altitude of 817 km, with a 2600 km wide swath, providing near-daily global coverage and overpass local time at ascending node of 13:30 (repeat cycle of 17 days). The spatial resolution at nadir, originally of 3.5×7 km^2 (across-track × along-track) has been refined to 3.5×5.5 km^2 on 6 August 2019.

The TROPOMI ALH product focuses on the retrieval of vertically localized aerosol layers in the free troposphere, such as desert dust, biomass burning aerosol, or volcanic ash plumes. It can therefore provide accurate values to the modelling community by improving air quality forecasting and radiative forcing studies. The height of such layers is retrieved for cloud-free conditions. Retrieval of the aerosol height is based on the absorption in the Oxygen-A band in the near-infrared wavelength range (759-770 nm) and assumes a single aerosol layer with 50 hPa thickness. This is an important simplification to note when comparing with other satellites and ground-based lidar profiles (e.g. from EARLINET), since these lidar profiles have the capability to detect multiple aerosol layers. The Oxygen-A band can provide altitude information on scattering layers (clouds or aerosol) from the troposphere up to the stratosphere. The TROPOMI Aerosol Layer Height (AER_LH) algorithm was developed by the Royal Netherlands Meteorological Institute (KNMI;Sanders et al., 2015; Nanda et al., 2018 Nanda et al., 2020) and is a part of the TROPOMI operational algorithm suite. We used S5P L2_AER_LH data covering the time period from May 2018 till Sep 2021. In brief, several quality control filters are applied in the TROPOMI L2 dataset, following the filtering proposed for ALH product (Nanda et al. 2020; their Table 1). Detailed description of the product can be found in appropriate versions of the Product User Manual (PUM; Apituley et al., 2021) and Algorithm Theoretical Basis Document (ATBD; de Graaf et al., 2021).

Additionally, we use the operational UV Aerosol Index (UVAI) TROPOMI product (Stein-Zweers et al., 2021) to examine the consistency of AER_LH products over the selected domain. The UVAI is an air quality product derived from the TOA reflectance spectra and is widely used as an indicator for the presence of absorbing aerosols in the atmosphere. The UVAI is based on spectral contrast in the UV spectral range for a given wavelength pair, where the difference between the observed reflectance and the modelled clear-sky reflectance results in a residual value. It should be noted that the UVAI TROPOMI product, is calculated for two wavelength

https://doi.org/10.5194/acp-2022-412
Preprint. Discussion started: 18 July 2022

pairs, 354/388 nm and 340/380nm with the first one allowing a direct comparison to the UVAI from the OMI/Aura instrument. Positive values indicate the presence of absorbing aerosols, such as dust, smoke, or volcanic ash. Clouds yield near-zero residual values and negative residual values can be indicative of the presence of non-absorbing aerosols, as shown by sensitivity studies of the UVAI (e.g. de Graaf et al., 2005).

2.3 Validation methodology and collocation criteria

In this section, we present in detail the basic principle of the validation method of the TROPOMI ALH product. The methodology is demonstrated using a selected number of collocated cases of TROPOMI overpasses over selected EARLINET lidar stations located around the Mediterranean Basin for the period June 2018 to September 2021. The approach followed is based on the previous expertise and methodology that have been developed using EARLINET observations for the GOME2/MetOp validation activities (Michailidis et al., 2021). At present, seven EARLINET stations operating at 1064 nm (or 532 nm) channel contribute to this study (**Figure 1**). To construct a validation dataset with statistical significance, ground-based lidar measurements from first need to be collected and collocated with TROPOMI observations. The profiles from different types of lidar instruments have to be interpreted in terms of their ALH profile parameter (e.g. height of the assumed single aerosol layer) in a consistent way to reduce mismatch errors due to the significant different horizontal sensitivity between TROPOMI and lidar measurements. Individual TROPOMI pixels are averaged over a selected radius around the lidar stations. Taking into account the recommendations of the previous comparison studies (Griffin et al., 2020; Nanda et al., 2020; Chen et al., 2021), the selection of data and the comparison between TROPOMI and EARLINET aerosol heights proceed through the following steps, also shown as a flowchart in **Figure A 1** for each date:

1. Create a list of TROPOMI overpass swaths that are within the region of interest (EARLINET stations).
2. Identify the closest TROPOMI pixels (within a radius of 150km) around the EARLINET stations in time and space. A maximum time difference of ±4h is allowed between collocation pairs. This choice is a compromise to obtain a significant number of coincidences between two datasets. A shorter time and spatial coincidence criterion significantly decreases the numbers of sampled collocated days.
3. For each ground-based measurement, the spatially averaged TROPOMI pixels in a radius of 150 km, were selected for the comparison study.
4. As input to the validation processing, we use the lidar backscatter coefficient profiles mainly at 1064 nm (or 532 nm), analyzed by the SCC (D'Amico et al., 2015; 2016) for quality-assured measurements and TROPOMI Level-2 ALH product.
5. In order to make an accurate validation analysis we apply quality screening flags (Nanda et al., 2020; their Table 1), to eliminate samples and layers that were detected or classified with very low confidence or that contained untrustworthy height retrievals. Finally, TROPOMI and EARLINET observations have been

https://doi.org/10.5194/acp-2022-412
Preprint. Discussion started: 18 July 2022


Atmospheric Chemistry and Physics Discussions

carefully checked, and atmospheric conditions have been studied to ensure that cloud-scenes are excluded from the compared datasets.

The real aerosol height may be also described in terms of layer boundaries or by the full vertical profile. In this study, we make use of the weighted-backscatter height (ALH_{bsc}), calculated as the center of mass (Z_{COM}) on backscatter (bsc) profile, based on the methodology described in Mona et al. (2006). This height parameter is an important indicator for vertical profiles that gives in a single number an indication of the altitude of the aerosol distribution. For example, in cases where a single aerosol layer is present in the atmosphere, the ALH_{bsc} gives an indication of its mean altitude; in case of multiple layers however, the ALHbsc could be located in areas without any considerable aerosol load. In addition ALH_{ext} is considered ideal for comparisons with aerosol layer height retrievals from passive remote sensing (e.g. TROPOMI/S5P, GOME-2/MetOp and upcoming Sentinel-4 & 5 missions). Information about the aerosol layer center of mass is useful because the characteristics of the detected layer can be distinguished at this altitude. Under the detection of a homogenous aerosol layer, the Z_{com} can be estimated as the mean altitude of the identified aerosol layer weighted by the altitude-dependent aerosol backscatter coefficient. In some cases, the aerosol vertical structure is very complicated because aerosol layers are present at different heights. For these cases, a total layer resulting from the multi-layered structure is considered for the calculation of mean optical parameters and integrated values. The weighted-backscatter altitude is estimated by the equation:

$$ALH_{bsc} = \frac{\int_{z_{i=1}}^{z=n} z_i \cdot \beta_{aer,i}(z)dz}{\int_{z_{i=1}}^{z=n} \beta_{aer,i}(z)dz} \qquad \text{(Equation 1)}$$

where $\beta_{aer,i}$ represents the aerosol backscatter coefficient ($Mm^{-1} \cdot sr^{-1}$) primarily at 1064 nm channel at level i and Z_i is the altitude (km) of level i for the aerosol profile signal. Based on the above equation, the layer height is calculated from backscatter profiles, symbolized as ALH_{bsc} (or $ALH_{EARLINET}$). The ALH_{bsc} represents an effective ALH weighted by the aerosol backscatter signal at each level and is the best parameter to compare with ALH as defined in the TROPOMI algorithm. In our work analysis, we applied Equation 1 to all lidar backscatter profiles collocated to TROPOMI measurements. In order to characterize the detected aerosol layers, in terms of their geometrical properties, parameters such as the layer base (Z_{BASE}), layer top (Z_{TOP}), layer thickness (L_{TH}) and center of mass (Z_{COM}), can be also calculated from the lidar signals.

Following the work proposed by Michailidis et al. (2021) for automatic layer detection, we also apply the WCT (Wavelet Covariance Transform) approach in order to check whether the TROPOMI retrieved ALH is sensitive to distinct layers rather than a representative effective layer from the whole profile. In this methodology, described in Appendix A2, all possible individual layers identified by the lidar observations are analysed autonomously, providing individual assessments on the height of the aerosol mass, and not a mean effective height from all layers as is extracted by Eq. 1. Hence, further below, a comparison is also given using the WCT formalism on the lidar profiles, from which the layer considered most optically significant is compared against

https://doi.org/10.5194/acp-2022-412
Preprint. Discussion started: 18 July 2022

Atmospheric Chemistry and Physics Discussions

TROPOMI ALH retrievals. In the case where more than one layers with a significant contribution to the optical thickness of the profile, an average value between these is calculated for the comparison against satellite height retrievals.

3 Validation Results and Discussion

Following the methodology summarized in **Section 2.3**, we performed a validation analysis using lidar data from 7 ground based EARLINET sites located across the Mediterranean, spatio-temporally collected with data from TROPOMI instrument aboard Sentinel-5P satellite. The results of this analysis are presented and discussed in detail in **Section 3.1**. Furthermore in **Section 3.2**, two selected representative cases are presented in detail, during extensive dust and smoke events over the Mediterranean Basin in order to illustrate strengths and limitations of TROPOMI ALH product.

3.1 Comparison of TROPOMI against EARLINET ALH

Here we present the first comparison between TROPOMI ALH and EARLINET measurements over the Mediterranean. The basic issue in this validation approach was the difficulty in identifying good spatiotemporal collocations between EARLINET lidar stations observations and TROPOMI/S5P overpasses. The TROPOMI AER_ALH retrievals over land surfaces is a challenge and strongly dependent on the surface albedo, with low accuracy for bright surfaces. First comparison results presented here confirm this. Overall, from the selected EARLINET stations across the Mediterranean, 34 coincident cases were found, checked and flagged for the comparison against TROPOMI retrievals. The collocated aerosol backscatter profiles at 1064nm from lidar level-2 products are used to calculate a ALH_{bsc} for the validation of TROPOMI ALH. The TROPOMI retrieval closest to the overpass time of TROPOMI are used in the validation for each day. The total available dataset is on the small side but suitable for the comparison study and general representativeness of the TROPOMI ALH product. For each selected satellite file, TROPOMI UVAI data were used to discriminate aerosol plumes from the background. We apply our validation process using satellite retrievals both over land and water surfaces to further demonstrate the known TROPOMI ALH issues over land. The surface reflectance for each pixel is derived after classifying the land and water surface based on the pixel location. Only a few data satellite points are available over the land and so a meaningful direct comparison over land only is not possible. Recall that over land the TROPOMI ALH product has decreased detection capabilities than over the sea surfaces since, over bright surfaces, the retrieval algorithm becomes increasingly sensitive to errors in the surface albedo features. The mean maximum layer heights for all cases are, on average, 3.65 km (ranging between 1.73 and 9.30 km) and 2.63 km (ranging between 1.12 and 6.51 km) for EARLINET and TROPOMI, respectively. These height ranges are reduced when land pixels are included (**Table *2***).

Table *2*. Layer height retrievals (min, max and average) of the EARLINET and TROPOMI ALH collocations.

https://doi.org/10.5194/acp-2022-412
Preprint. Discussion started: 18 July 2022

Atmospheric Chemistry and Physics Discussions

Instrument	Min height (km)	Max height (km)	Average height (km)
TROPOMI (ocean)	1.12	6.51	2.63±1.24
TROPOMI (land/ocean)	0.90	5.09	2.19±0.83
EARLINET	1.73	9.30	3.65±1.90

The agreement between the TROPOMI-EARLINET datasets was quantified by several evaluation metrics, including the number of collocations (N), the linear correlation coefficient (R), the slope (a) and intercept (b) of the linear regression, the root mean square error (RMSE), and the mean bias (MB), representing their mean difference. By defining a weighted height from EARLINET aerosol backscatter profile products (ALH_{bsc}), the quantitative validation at pixels over the selected EARLINET stations illustrates that TROPOMI ALH is consistent with ALH_{bsc}, with a high correlation coefficient R=0.89 and mean bias −1.017 ± 0.96km over ocean pixels and R=0.59 and −1.46±1.57km over both land/ocean pixels, respectively. **Figure *2*** shows the scatterplot of TROPOMI ALH against EARLINET ALH_{bsc} for all the common cases used for the intercomparison. Ocean-only S5P pixel comparisons are shown in **Figure *2*** (upper) and both S5P ocean and land pixels are shown in **Figure *2*** (center). The yellow solid line is the linear fit line between the datasets. The error bars represent the corresponding spatial standard deviation of TROPOMI pixels within 150km of the EARLINET sites. The colour scale indicates the averaged TROPOMI aerosol index values.

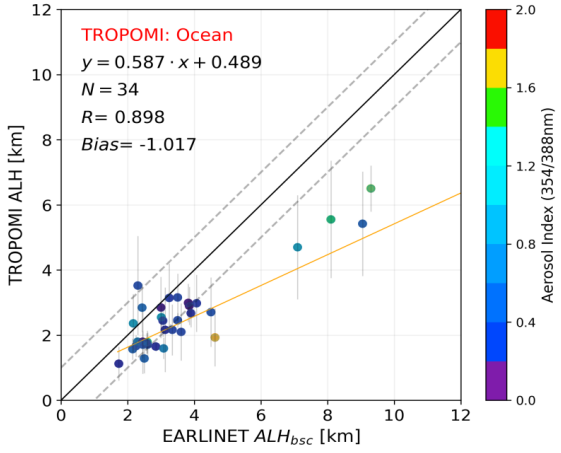

https://doi.org/10.5194/acp-2022-412
Preprint. Discussion started: 18 July 2022

Atmospheric Chemistry and Physics Discussions

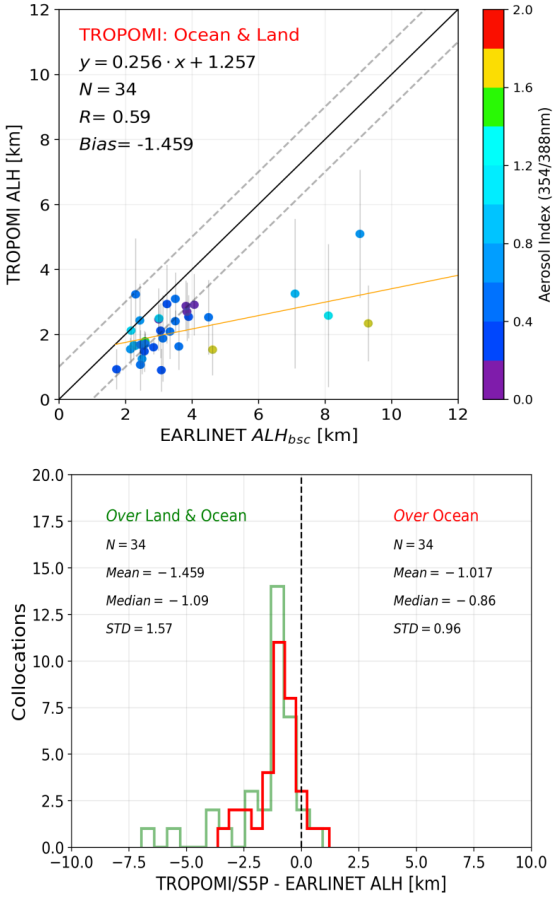

Figure *2*. Scatterplots of TROPOMI against EARLINET data: (upper) TROPOMI pixels over ocean and (center) over ocean and land. The color of each scatter point indicates the TROPOMI retrieved UVAI values, and the error bars of each scatter indicate the spatial variability of the averaged TROPOMI ALH pixels. (Bottom) Histogram of the differences between TROPOMI and EARLINET datasets, in red over the ocean pixels and in green for both ocean and land pixels.

From these scatter plots, it can be noted that there are two different point clusters which represent two different aerosol events. The cluster with the low aerosol layer heights (upper and center in Figure 2) represents the dust episodes, while the high aerosol loads (upper and center in Figure 2) represent the four collocated cases associated to smoke events over the west, central and east Mediterranean which originated from the California forest fires. These cases have thin and well defined layer structure, with no significant contribution from lower layers, apart from the Planetary Boundary Layer (PBL) structure. Overall, the TROPOMI ALH retrievals are systematically lower than the compared lidar height in both clusters. This can be seen also in **Figure *2*** (bottom) which presents histogram plots of absolute differences. The magnitude of the mean height difference is smallest when only ocean pixels are included in the comparison with the EARLINET and increases when compared with land/ocean pixels. Many factors can play a role in this apparent disagreement between TROPOMI retrievals

https://doi.org/10.5194/acp-2022-412
Preprint. Discussion started: 18 July 2022

over land and sea including that high surface albedos negatively influence the ALH, biasing the ALH towards the surface. The accompanied related statistic metrics are summarized in **Table *3***.

Table *3*. Statistics of the comparison between TROPOMI and EARLINET ALH datasets.

TROPOMI pixels	N[a]	R[b]	Slope[c]	Y[d]	MB[e]	RMSE[f]
Ocean	34	0.90	0.58	0.49	-1.01km	1.39km
Ocean and land	34	0.59	0.25	1.26	-1.46km	2.12km

[a]Number of collocations,[b]Correlation coefficient, [c]Slope from linear regression fit , [d]Y-intercept of linear regression fit, [e]Mean bias, [f]Root mean square error

We further assessed the capabilities of the TROPOMI ALH product compared with well-defined layers obtained using the WCT formalism over both land and water surfaces. A case study explaining this methodology is presented in Appendix A2 and detailed results with the WCT techniques are shown also for the three case studies discussed further on in this paper. Using this approach to define the lidar aerosol layer height we also found similar results, namely a high correlation coefficient R=0.87 and mean bias of −1.41±1.51km over ocean pixels and R=0.56 and mean bias of −1.85±2.1km over both land/ocean pixels. For typical single-layered aerosol cases, the differences between the TROPOMI and lidar retrieved heights are generally low using either the formal methodology presented with Eq. 1 or the WCT technique. Larger differences are observed for multi-layered aerosol events, possibly due to the limited sensitivity of the passive sensors to such cases. Using the more evolved WCT method for analysing the lidar profiles for validating purposes adds value in the case of multi-layer structures, as shown further below. However, to refine this automated technique, more cases have to be analysed in the future, as these become available.

3.2 Case studies: Analysis and results

Three typical days with sufficient aerosol load over Mediterranean were selected to illustrate the performance of the TROPOMI ALH product over scenes with strong aerosol load. These cases refer to Antikythera, Evora and Potenza lidar observations during extended dust and smoke events. The selected cases include: (a) a Saharan dust outbreak over eastern Mediterranean region on 22nd of June 2021 and (b) a smoke aerosol plume transported during 4 days between the 24th and the 27th of October 2020, originated from the large wildfire episodes in the California region (N. America).

3.2.1 Dust case over Eastern Mediterranean: 22 June 2021, PANGEA observatory (Greece)

On the 22nd of June the Eastern Mediterranean was affected by a strong dust episode originated from North Africa. On this day, the TROPOMI overpass over Greece is between ~10:00 and 11:00 UTC. A lofted layer of dust was also clearly observed by the PollyXT system at PANGEA Antikythera station on the same day. The

https://doi.org/10.5194/acp-2022-412
Preprint. Discussion started: 18 July 2022

Atmospheric Chemistry and Physics Discussions

PANGEA observatory of NOA on the remote island of Antikythera is located across the travel path of different air masses, providing continuous monitoring of essential climate variables in the Eastern Mediterranean (Kampouri et al., 2021). A PollyXT NOA lidar (Engelmann et al., 2016) is installed in the PANGEA observations in Antikythera since August 2018. This multi-wavelength system is part of the EARLINET community, with 24/7 operational capabilities, providing vertical distributions of aerosol properties at different wavelengths. The dust plume can clearly be seen in **Figure *3*** (left), over Greece from theVIIRS/Suomi-NPP true color image for this day (VIIRS images are generated from https://wvs.earthdata.nasa.gov/; last access: 1 May 2022). With the red star symbol the PANGEA lidar station at Antikythera is depicted. **Figure *3*** (center) and **Figure *3*** (right) show the TROPOMI ALH and UVAI product retrievals, during the investigated dust episode. Comparing the TROPOMI product maps to the VIIRS image, it is obvious that the large positive UVAI pixels and elevated aerosol layers are located at the detected plumes.

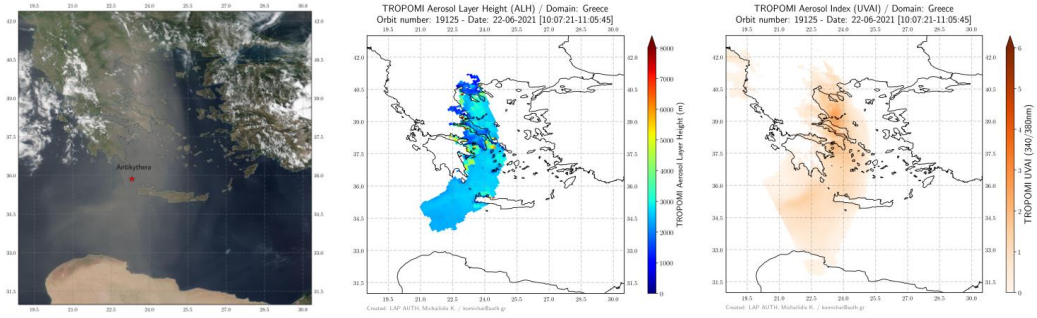

Figure *3*. (Left) VIIRS Suomi-NPP True color image from the NASA Worldview application (https://worldview.earthdata.nasa.gov, last access: 5 March 2022) on the 22nd June 2021. (Center) TROPOMI ALH and (right) TROPOMI UVAI over Greece. The red star indicates the position of the Antikythera lidar station.

Figure 4 (left) presents the total attenuated backscatter signal time-series for the PollyXT at 1064nm, over Antikythera between 10:00-13:00 UTC on this day. A notable and homogeneous layer can be identified throughout the day below 5 km. The aerosol load is mainly between 500 and 4500 m and the sky above the site is cloud-free during the TROPOMI overpass time (thick red line). Additionally, in order to verify the origin of the detected aerosol layers, we calculated back-trajectories by using the HYSPLIT model (Hybrid Single-Particle Langrangian Integrated Trajectory; available online: last access: 01 May 2022; Stein et al. 2015). The temporal evolution of 3-day backward trajectories, for the 21st of June, for selected arrival heights (2000m (red), 3500m (green) and 5000m (yellow)) is illustrated in **Figure 4** (right). As can be seen, the air masses arrived over Antikythera station follow a pattern originating from North-western Africa.

https://doi.org/10.5194/acp-2022-412
Preprint. Discussion started: 18 July 2022

Atmospheric Chemistry and Physics Discussions

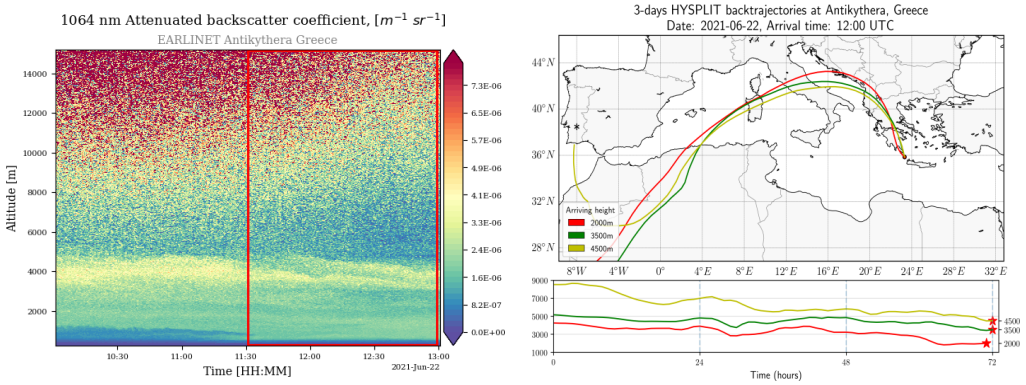

Figure 4. (Left) Temporal evolution of the total attenuated backscatter signal from the PANGEA PollyXT at 1064nm and (right) 3-day back-trajectories arriving at Antikythera, Greece on 22 June 2021 at 12:00 (HYSPLIT accessible at www.ready.noaa.gov).

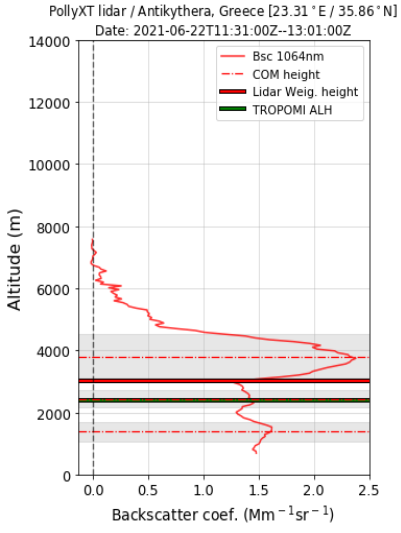

Figure 5. Lidar backscatter profile at 1064nm (ALH_{bsc}, red line) at Antikythera, Greece on 22 June 2021. The Lidar weighted aerosol height by Eq. 1 is shown as a thick red line. The calculated center-of-mass (COM) of the two identified layers are shown as dash-dot red lineσ and their thickness as the grey areas. The TROPOMI mean ALH is given as the thick green line.

For this event, the TROPOMI ALH spatially averaged values and the EARLINET temporally averaged backscatter coefficient profiles (between 11:30-13:00 UTC) are qualitatively compared in **Figure 5**. Two optically thin layers with a thickness of less than 300 m were detected, with centers of mass shown as the red dash-dot lines and their spread as the grey areas. TROPOMI detects this layer at 2550m while the calculated ALH_{bsc} from applying Eq. 1 to the lidar profiles places it at 3010m. An agreement within 500m between the satellite and ground-based lidar systems is hence found for this clear aerosol scene, within the target requirement for the TROPOMI ALH product (ATBD; de Graaf et al., 2021). The presented case study indicates that, under cloud-free conditions where homogeneous aerosol layers are developed, the mean ALH value retrieved by the

https://doi.org/10.5194/acp-2022-412
Preprint. Discussion started: 18 July 2022


Atmospheric Chemistry and Physics Discussions

TROPOMI is in excellent agreement with the calculated ALH_{bsc} from the lidar profile, confirming the findings of Griffin et al. (2020) and Nanda et al. (2020).

Using the WCT algorithm on the β_{aer} profile at 1064 nm, we can also extract the geometrical properties of detected layers. Once the top and the base of the aerosol layer are identified, the Z_{com} and optical properties of each aerosol layer can be also estimated. In this way, we can also investigate if there are strong variations in the b_{aer} (or b_{sc}), which may lead to an identification of a separate layer. For the predominant thick layer (upper layer shown in **Figure 5**), the retrieved geometric properties are: layer base (3150 m), layer top (4350 m), layer thickness (2200 m), layer center of mass (4000 m). This example amply demonstrates that when using the WCT technique as a reference, in the presence of two layers with different spreads, the best agreement with the satellite estimate is not necessarily found for the optically thickest one. The representativeness of the TROPOMI ALH when multiple layers are present is undoubtedly an issue of further investigation in the future.

3.2.2 Smoke advection over the Mediterranean from Californian fires

In mid-October 2020, a series of wildfires took place in Northern California resulting in thousands of square kilometers of boreal forest being burned and causing a huge amount of smoke to enter the atmosphere. The emissions caused extreme air pollution conditions with poor visibility throughout the area for several days. The TROPOMI sensor has been monitoring these wildfires, and recently tracked the smoke as it travelled all the way across North America and the Atlantic Ocean to arrive in Mediterranean (Baars et al., 2021; Ansmann et al., 2021). These smoke aerosol layers were transported from the US west coast towards Europe within 4-5 days. The smoke arrived over the Iberian Peninsula (IP) in southwestern Europe on 24 October (**Figure *6***a), just in time for a regular overpass of the TROPOMI over Iberian Peninsula. As the plume was transported along the Mediterranean, it was detected over southern Italy and Greece, shown in the true color images from VIIRS/Suomi-NPP (**Figure *6***b to d). The S5P trails behind Suomi-NPP by 3.5 min in Local Time Ascending Node, allowing its swath to remain within the scene observed by Suomi-NPP. We have to note here that the ALH is very sensitive to cloud contamination as aerosols and clouds can be difficult to distinguish. In general, the VIIRS cloud mask has good performance for pixels covered by aerosol plumes, but in many cases where very thick layers are detected the cloud mask can misclassify the retrievals pixels as cloudy pixels with high cloud fraction. The equivalent daily TROPOMI UVAI and ALH product retrievals are presented in **Figure *7*** and **Figure *8***, respectively. The detected smoke plumes are highlighted by large positive values of UVAI, which are in contrast to clouds that typically exhibit a negative UVAI or/and close to zero (Torres et al., 1998).

https://doi.org/10.5194/acp-2022-412
Preprint. Discussion started: 18 July 2022

Atmospheric Chemistry and Physics Discussions

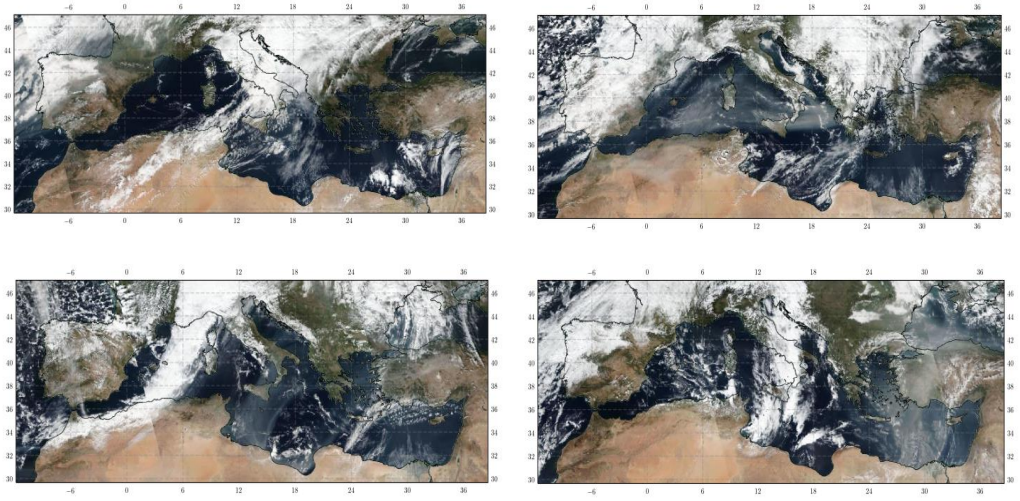

Figure 6. VIIRS-Suomi NPP True color images for the four smoke scenes on 24-27 October 2020 (Maps are generated from NASA Worldview Snapshots: https://wvs.earthdata.nasa.gov/, last access: 5 March 2022)

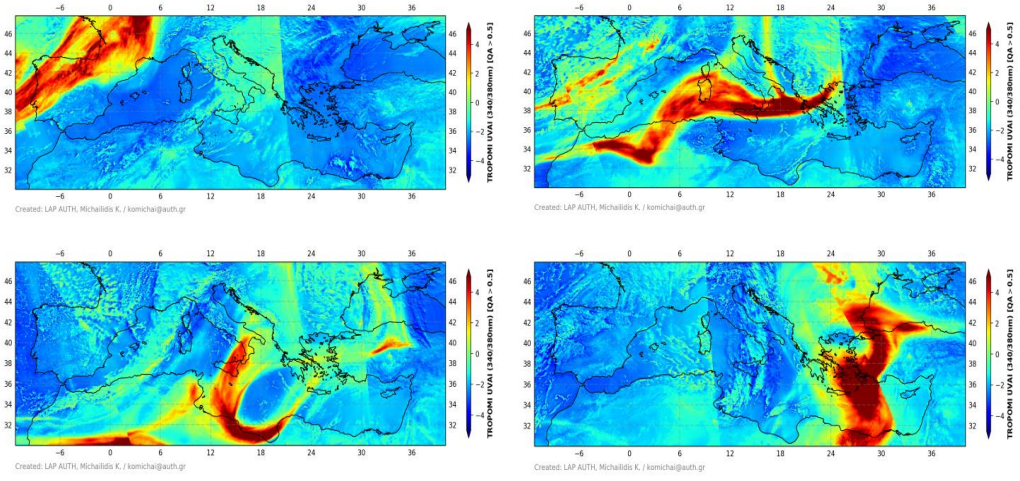

Figure 7. TROPOMI UV aerosol index (UVAI) retrievals during the smoke plume transport over the Mediterranean, during 24-27 October 2020.

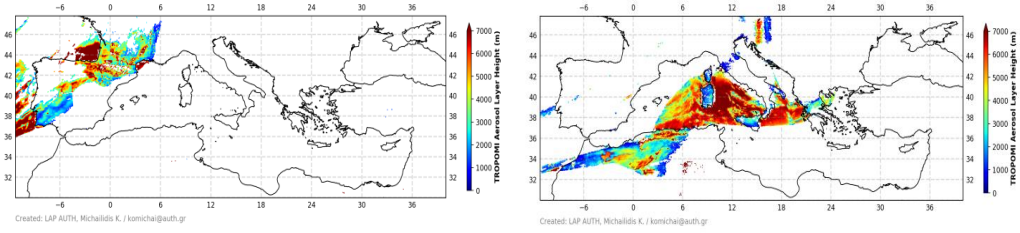

https://doi.org/10.5194/acp-2022-412
Preprint. Discussion started: 18 July 2022

Atmospheric Chemistry and Physics Discussions

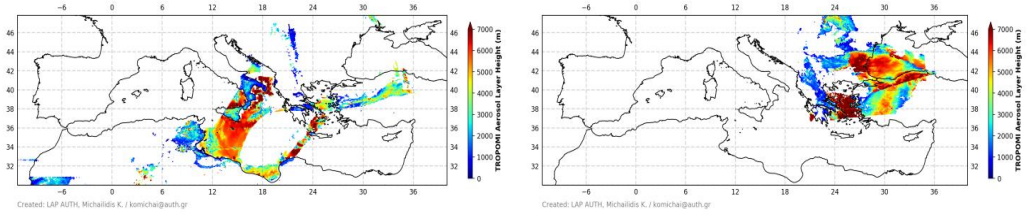

Figure *8*. TROPOMI Aerosol Layer Height (ALH) retrievals during the smoke plume transport over the Mediterranean, during 24-27 October 2020.

- **Smoke case over western Mediterranean: 24 October 2020, Évora (Portugal)**

On 24 October 2020, during the Suomi-NPP satellite overpass, the VIIRS sensor captured the true color image (**Figure 9**, left) showing a large amount of smoke plumes in the western half of the Iberian Peninsula (IP), particularly in the north-western areas facing the Atlantic Ocean. The selected scene is also strongly affected by the presence of clouds. TROPOMI overpassed Évora around 12:30 UTC on this day and recorded very high values related to UVAI values (>5) (**Figure 9**, right) as well as elevated aerosol plumes corresponding to high ALH values (**Figure 9**, center). The maximum altitude in the AER_LH data is about ~8 km. The white spaces in the TROPOMI product maps indicate no valid TROPOMI retrievals over these areas. On October 26th, 2020, a smoke plume originated from North American fires spread towards the central Mediterranean.

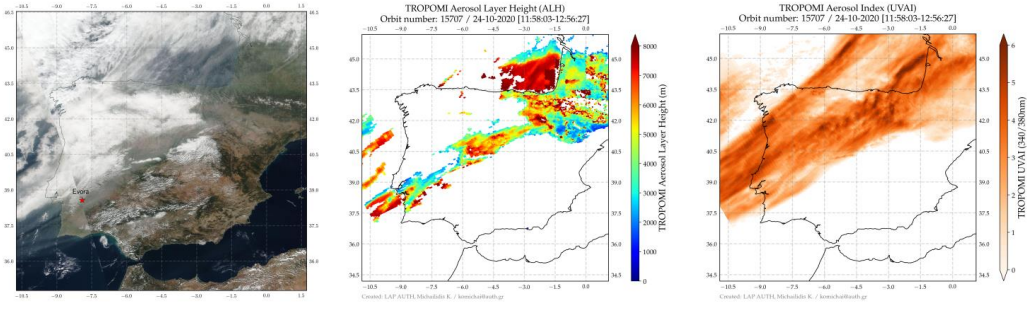

Figure 9. (Left) VIIRS Suomi-NPP True color image from the NASA Worldview application (https://worldview.earthdata.nasa.gov, last access: 5 March 2022) on 24 October 2020 over the Iberian Peninsula, capture the smoke plume. The red star indicates the position of the Potenza lidar station, (center) TROPOMI ALH and (right) UVAI retrievals at 340/380nm pair. Missing ALH pixels are flagged by a cloud or have negative AI values.

Figure 10 (left) illustrates the temporal evolution of the observed aerosol plume by means of the time–height cross section of the 1064 nm total attenuated backscatter coefficient for the time period from 12:00 UTC to 17:55 UTC on the 24th of October. As observed in these timeseries obtained from PollyNet (https://polly.tropos.de/, last access: 01 May 2022), a significant particle load is detected after 11:00UTC, at 10-12km approximately. The red dashed box indicates the temporal averaging of these lidar signals close to the S5P overpass time. The Portable Aerosol and Cloud Lidar (PAOLI) installed at the Évora Atmospheric Sciences

https://doi.org/10.5194/acp-2022-412
Preprint. Discussion started: 18 July 2022

Atmospheric Chemistry and Physics Discussions

Observatory (EVASO) (38.57°N, 7.91°W; 293 m a.s.l.) is a multiwavelength Raman lidar of the type Polly^{XT} (Baars et al. 2016; Salgueiro et al., 2021) part of the European Aerosol Research Lidar Network (EARLINET). Backward trajectories **Figure 10** (right) generated with the HYSPLIT model were used to determine the origin of the air masses carrying aerosol plumes arriving at the Évora site at the relevant heights (7500, 9500 and 480 11500m). They confirmed that the relevant air masses came from areas over North American, Californian forest fires detected by VIIRS.

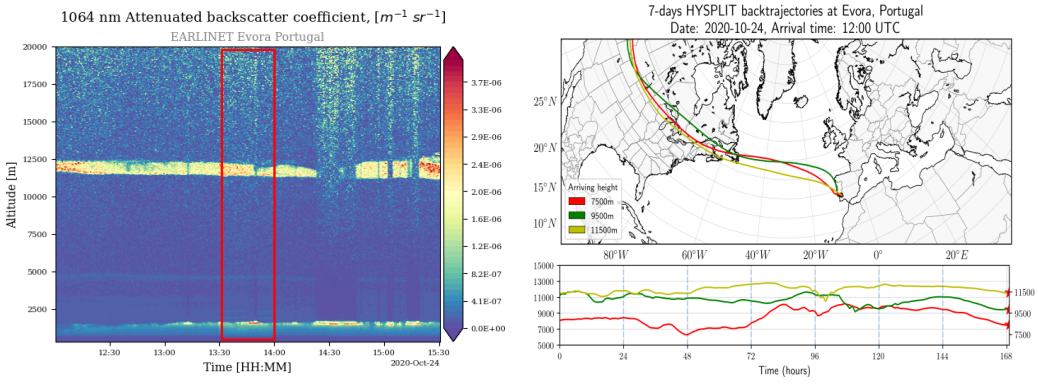

Figure 10. (Left) Temporal evolution of the total attenuated backscatter signal from the PAOLI PollyXT lidar system at 1064nm showing the detection of the smoke cloud. (Right) 7-day HYSPLIT back-trajectories arriving at Évora, Portugal on 24 October 2020 at 12:00.

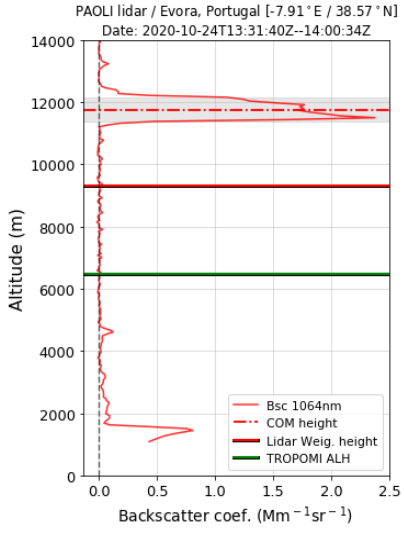

485 **Figure 11**. As per **Figure 5** for the PAOLI lidar observation on 24 October 2020.

In **Figure 11** the retrieved vertical profile of the observations with PollyXTlidar is presented. The temporally closest backscatter profile is used to extract the ALH_{bsc} and compare against the TROPOMI ALH retrievals. The average backscatter profile at 1064 nm, for the time period from 13:30 to 14:00 UTC on 24 October 2020 is shown. The TROPOMI observations report an averaged layer at 6300m, while the calculated ALH_{bsc}

https://doi.org/10.5194/acp-2022-412
Preprint. Discussion started: 18 July 2022

Atmospheric Chemistry and Physics Discussions

(following Eq. 1) from the lidar profile places it at 9300m. As above, we also applied the WCT method on the backscatter vertical profile, in order to extract the aerosol boundaries of the detected aerosol layers in automatic way. The WCT techniques also reveals a clear single layer between 11000 and 12500m with maximum backscatter value ~1.8 $Mm^{-1}sr^{-1}$ and center of layer mass at 11800m. For this case, we note the large discrepancy of both lidar layer identification techniques and the TROPOMI ALH whose reasons warrant further investigation in the future.

- **Smoke case over central Mediterranean: 26 October 2020, Potenza (Italy)**

On October 26th, the same smoke plume spread towards the central Mediterranean due to the easterly prevailing winds across Italy and Greece. In this sub-section, we present a case study within this smoke episode, over the Potenza lidar station in Italy for the 26th of October 2020. A significant aerosol load is observed mainly over the south of Italy. The true color image (**Figure 12**, left) captured by VIIRS aboard Suomi-NPP, provides the context for the retrievals shown next. The location of the smoke plume is clearly seen in the TROPOMI ALH and UVAI images (**Figure 12,** center & right) during the Sentinel-5P overpass between 11:20-12:20 UTC. The TROPOMI UVAI shows a wide range of values with several patches with no retrievals due to the presence of clouds.

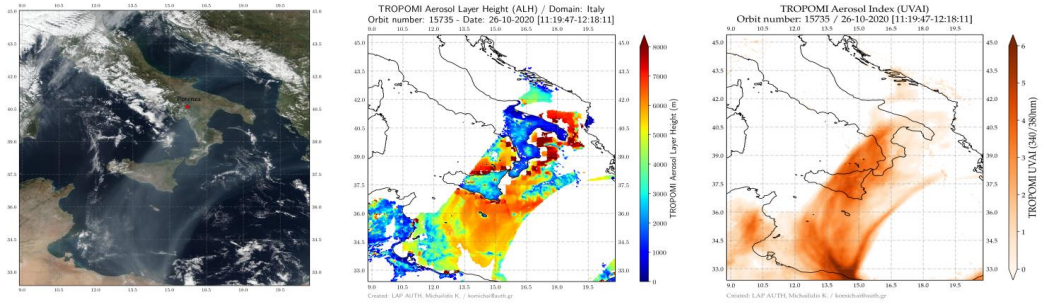

Figure 12. (Left) VIIRS Suomi-NPP True color image from the NASA Worldview application (https://worldview.earthdata.nasa.gov, last access: 5 March 2022) on 26 October 2020 over central Mediterranean, capture the smoke plume. The red star indicates the position of the Potenza lidar station. (Center) TROPOMI ALH and (right) UVAI retrievals. Missing ALH pixels are flagged by a cloud or have negative AI values.

The event is extensively recorded on October, 26th, 2020 at the Potenza lidar station. MUSA is the lidar system (Madonna et al., 2011) deployed at CNR-IMAA Atmospheric Observatory (CIAO) in Potenza (40.60°N, 15.72°E, 760 m a.s.l.). **Figure 13** (left) shows the total attenuated backscatter time-series at 1064 nm measured by the MUSA system during the smoke event. The lidar observations started on 26 October 2020 at 10:00 UTC and lasted almost continuously until 13:30 UTC. The red dashed box indicates the temporal averaging of the lidar signals (10:00–11:30 UTC) close to the TROPOMI/S5P overpass time. Multilayer structures were found and smoke particles appeared in the free troposphere, between 6000 and 11000 km above sea level (a.s.l.). The intense part of the smoke plume is located about 300 km south of the Potenza EARLINET station where the

https://doi.org/10.5194/acp-2022-412
Preprint. Discussion started: 18 July 2022

Atmospheric Chemistry and Physics Discussions

520 atmospheric conditions are different with different TROPOMI retrievals from above the station. The temporal evolution of 7-day backward trajectories, for this day (arrival heights: 7500 (red), 9500 (green) and 11500 m (yellow) is illustrated in **Figure 13** (right). As can be seen, the air masses which arrived over Potenza station seem to originate from N. America, following an almost straight route path towards Italy.

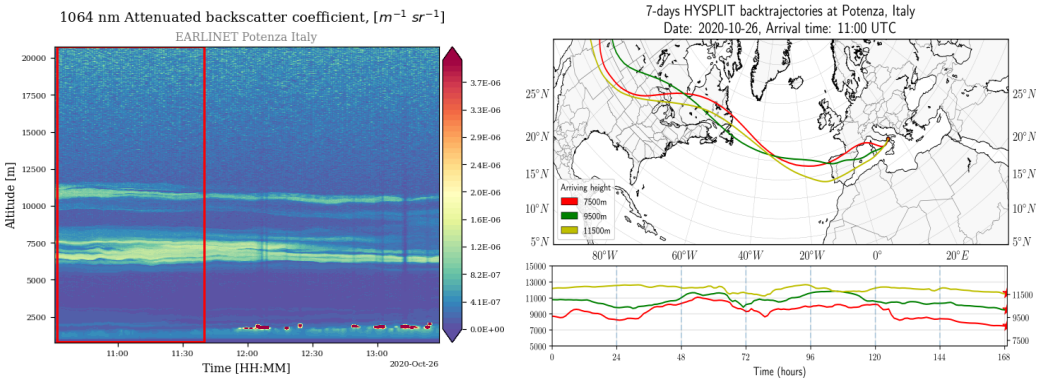

Figure 13. (Left) Temporal evolution of the total attenuated backscatter signal from the MUSA lidar system at 1064nm
525 showing the detection of the smoke cloud. (Right) 7-day HYSPLIT back-trajectories arriving at Potenza, Italy on 24 October 2020 at 11:00.

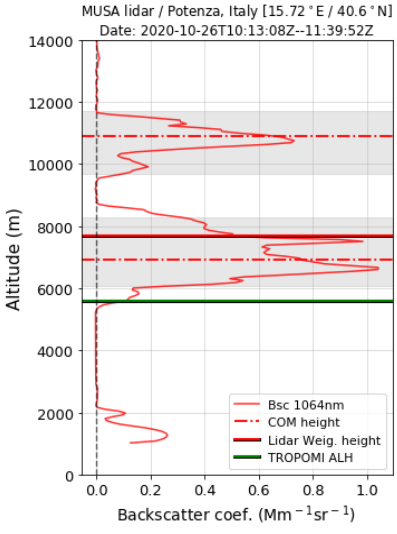

Figure 14. Same as **Figure 5** for the MUSA lidar observations on 26 October 2020.

In **Figure 14** the retrieved vertical profile of the observations with MUSA lidar is presented. The closest in time backscatter profile is used in order to extract the ALH_{bsc} and compare against TROPOMI ALH retrievals. The
530 averaged backscatter profile at 1064 nm, for the time period from 10:15 to 11:40 UTC on 24 October 2020 is shown. Two optical elevated thick layers with a thickness of ~2km were detected with TROPOMI detecting this layer at 5650m while the calculated ALH_{bsc}, from applying Eq. 1 on the lidar profile, places it at 7800m. For

https://doi.org/10.5194/acp-2022-412
Preprint. Discussion started: 18 July 2022

this case which shows two well-developed layers, the retrieved geometric properties by applying the WCT technique place the first detected layer at 7150m and the second at 11070m, also with thickness of ~2km. As previously, we also note here a discrepancy between both lidar aerosol heights and the satellite estimation of the aerosol height. Clearly, the AER_LH is placed much lower than both calculated altitude of the lidar profile. The exact reason for the much lower altitude retrieved by the AER_LH algorithm is not clear, however we should note that the AER_LH algorithm was not created to retrieve ALH at such low air pressures. The ALH pixels over Italy show clear outliers, with very low reported heights, along the inland region. All these pixels over land seem to result in an ALH very close to the ground. This case of very high altitude smoke from intense biomass burning in North America in 2020 shows a notable difference with lidar measurements, revealing a possible limitation of the current operational S5P L2_AER_LH product.

4 Summary and Conclusions

The TROPOMI Aerosol Layer Height (ALH) is a new and unique product providing global observations of aerosol height. TROPOMI aerosol layer heights can add value to the modelling communities by improving air quality forecasting and radiative forcing studies. Aerosol plume heights from TROPOMI have the advantage of daily global coverage. This is the first work in which TROPOMI ALH retrievals are validated against EARLINET lidar observations and the results provide an early evaluation of their applicability for monitoring aerosol height levels in a large area such as Mediterranean and Europe. This paper presents a cross-comparison analysis between TROPOMI and EARLINET data and provides a simple and well-developed methodology for comparing these different datasets. Lidar instruments retrieve the vertical backscatter coefficient, which is not directly comparable to the TROPOMI ALH product. Thus, the weighted-backscatter height (ALH_{bsc}) has to be calculated from the available backscatter profiles in the frame of this study. The Mediterranean basin is an ideal test environment for ALH features during extreme events. Dust transport is typical for the Mediterranean whereas smoke plumes in the tropopause/stratosphere are rare. However, due to the product limitations over the land only sea pixels have been selected into the analysis study. Coincidences within a 150 km radius from the lidar station are used for direct observations, with a maximum of 4h time difference. All the input datasets considered in the study have been previously pre-processed at high resolution by using the EARLINET Single Calculus Chain (SCC). Overall, for 7 selected EARLINET stations across the Mediterranean, 34 coincident aerosol cases were found during the time period June 2018 - September 2021, for the comparison against satellite retrievals. The statistical results show the ability of the TROPOMI instrument to detect aerosol layers under cloud-free atmospheric conditions with significant aerosol load, such as dust and smoke plumes.

Despite the different measuring concept that two instruments used for retrievals (passive & active), a good agreement was found between TROPOMI retrievals and ground-based lidar measurements, demonstrating that TROPOMI has a quite promising potential for the characterization of the aerosol vertical distributions on a

https://doi.org/10.5194/acp-2022-412
Preprint. Discussion started: 18 July 2022


Atmospheric Chemistry and Physics Discussions

global scale. By defining a backscatter-weighted aerosol height from EARLINET aerosol backscatter profile products (ALH_{bsc}), the quantitative validation at pixels over the selected EARLINET stations illustrates that TROPOMI ALH is consistent with ALH_{bsc}, with a high correlation coefficient R=0.91 (R=0.59) and a mean bias about −1.02 ± 0.96 km (−1.46 ± 1.57 km) over ocean and ocean/land pixels respectively. It appears that aerosol layer altitudes retrieved from TROPOMI are systematically lower than altitudes from the lidar retrievals. Our findings are in a good agreement with other TROPOMI ALH validation studies. Nanda et al. (2020) and Chen et al. (2021) discuss the challenges associated with the validation of TROPOMI ALH. These challenges arise mainly from the large spatio-temporal variability of aerosols, the dependency of the products on different geophysical parameters (e.g. surface albedo) and different instrument sensitivities. The target requirement on accuracy and precision of retrieved aerosol layer height is 0.5 km or 50 hPa; the threshold requirement is 1 km or 100 hPa. Overall, our results testify that the TROPOMI product complies with the S5P mission requirements.

The Wavelet Covariance Transform method was also applied on the ground-based lidar profiles so as to to quantify the effect of multi-layer structures on the comparisons between TROPOMI and lidar aerosol layer height. This method provides better insight as to the altitude ranges that the two instruments are sensitive to, however more case studies need to be analyzed in detail to draw conclusions concerning to which sensed layer the TROPOMI algorithm is more sensitive to.

This study highlights the importance of the synergistic use of active (ground-based lidars) and passive (satellite) observations and suggests a promising usage of TROPOMI ALH for understanding the details of the presence and transport of aerosol layers. The results presented here encourage the operational usage of the presented methodology approach in validation processes for satellite aerosol height products using lidar data from EARLINET. The increased availability of advanced and high quality-assured profiling data from EARLINET lidars will form a scientific background to improve performance of passive satellite sensors and lead to a better understanding of the role of the aerosol height on air-quality and the climate.

Data availability. The EARLINET data used in this study are available from the authors and upon registration from the EARLINET web page at https://data.earlinet.org/earlinet/login.zul (Pappalardo et al., 2014). TROPOMI ALH data are available from the S5P Pre-Operations Data Hub at https://s5phub.copernicus.eu/dhus, (last access: 01 May 2022).VIIRS/Suomi satellite data are available online at https://wvs.earthdata.nasa.gov, (last access: 01 May 2022). HYSPLIT data as described by Stein et al. (2015) can be found at https://www.ready.noaa.gov/HYSPLIT.php (last access: 01 May 2022)

Acknowledgments. We are grateful to all Co-PIs of the EARLINET sites used in this study for maintaining their instruments and providing their data to the community. This research was supported by data and services obtained from the PANhellenic Geophysical Observatory of Antikythera (PANGEA) of the National Observatory of Athens (NOA), Greece. We thank the PollyNet group, and especially Ronny Engelmann and Holger Baars, for their support during the development and operation of the PollyXT lidar of NOA. NOA team acknowledges the support of Stavros Niarchos Foundation (SNF). R-E M and AN acknowledge the ERATOSTHENES Centre of Excellence and the “EXCELSIOR” H2020 Widespread Teaming project that has received funding from the European Union's Horizon 2020 Research and Innovation programme under grant

agreement no. 857510 and from the Government of the Republic of Cyprus through the Directorate General for the European Programmes, Coordination and Development. DB, MJC and VS are co-funded by national Portuguese funds through FCT - Fundação para a Ciência e Tecnologia, I.P., in the framework of the ICT project with the references UIDB/04683/2020 and UIDP/04683/2020, as well as through TOMAQAPA (PTDC/CTAMET/29678/2017) and CILIFO (0753_CILIFO_5_E) projects.

Author contributions. KM carried out the processing of satellite and lidar measurements, prepared the figures of the manuscript and wrote the original draft of the manuscript with contributions from all co-authors **MEK** and **DB** were responsible for the methodology and conceptualization of the paper. **LM, NP, EM, IT, AG** perform the lidar measurements ensured the provision of the QA EARLINET data. **PV** and **MdG** worked on the development of the TROPOMI AER_LH product and were responsible for providing satellite data, detailed description of the product. **KM** contributed to the development of the automatic algorithm for the aerosol layer detection using lidar data. **AP, R-EM, MM, LAA, DB, MJC, VS, SR, SRP, MRP** reviewed the case studies of the selected EARLINET stations, as presented in the paper. All authors participated in scientific discussions on this study, reviewed &edited the manuscript during its preparation phase.

Financial support. This research has been supported by the "Panhellenic Infrastructure for Atmospheric Composition and Climate Change" project (grant no. MIS 5021516) which is implemented under the Action "Reinforcement of the Research and Innovation infrastructure" and co-financed by Greece and the European Union (European Regional Development Fund). The writing and editing of this paper was carried out as part of the ESA-funded Quality Assurance for Earth Observation (IDEAS-QA4EO) framework contract. The authors also acknowledge the financial support of the European Space Agency "Preparation and Operations of the Mission Performance Centre (MPC) for the Copernicus Sentinel-5 Precursor Satellite". The Limassol, Cyprus, observations have been supported by the SIROCCO project (grant no. EXCELLENCE/1216/0217) and AQ-SERVE project (INTEGRATED/0916/0016) co-funded by the Republic of Cyprus and the structural funds of the European Union for Cyprus through the Research and Innovation Foundation. The PollyXT-CYP lidar funded by the Federal Ministry of Education and Research (BMBF) via the PoLiCyTa project and its operation by the EU H2020 EXCELSIOR project. EM and VA were supported by the European Research Council (ERC) under Community's Horizon 2020 research and innovation framework programme-ERC grant agreement no. 725698 (D-TECT).

Competing interests. The authors declare that they have no conflict of interest.

References

Abril-Gago, J., Guerrero-Rascado, J. L., Costa, M. J., Bravo-Aranda, J. A., Sicard, M., Bermejo-Pantaleón, D., Bortoli, D., Granados-Muñoz, M. J., Rodríguez-Gómez, A., Muñoz-Porcar, C., Comerón, A., Ortiz-Amezcua, P., Salgueiro, V., Jiménez-Martín, M. M., and Alados-Arboledas, L.: Statistical validation of Aeolus L2A particle backscatter coefficient retrievals over ACTRIS/EARLINET stations on the Iberian Peninsula, Atmos. Chem. Phys., 22, 1425–1451, https://doi.org/10.5194/acp-22-1425-2022, 2022.

Amiridis, V., Balis, D. S., Giannakaki, E., Stohl, A., Kazadzis, S., Koukouli, M. E., and Zanis, P.: Optical characteristics of biomass burning aerosols over Southeastern Europe determined from UV-Raman lidar measurements, Atmos. Chem. Phys., 9, 2431–2440, https://doi.org/10.5194/acp-9-2431-2009, 2009.

Amodeo, A., D'Amico, G., Giunta, A., Papagiannopoulos, N., Papayannis, A., Argyrouli, A., Mylonaki, M., Tsaknakis, G., Kokkalis, P., Soupiona, R., and Tzanis, C.: ATHLI16: the ATHens lidar intercomparison campaign, in: 28th international laser radar conference, Bucharest, Romania, 25–30 June 2017, 176, 09008, https://doi.org/10.1051/epjconf/201817609008, 2018.

https://doi.org/10.5194/acp-2022-412
Preprint. Discussion started: 18 July 2022

Atmospheric Chemistry and Physics Discussions

Ansmann, A., Riebesell, M., Wandinger, U., Weitkamp, C., Voss, E., Lahmann, W., and Michaelis, W.: Combined Raman Elastic-Backscatter lidar for vertical profiling of moisture, aerosol extinction, backscatter, and lidar ratio, Appl. Phys. B, 55, 18–28, https://doi.org/10.1007/BF00348608, 1992.

Ansmann, A., Ohneiser, K., Mamouri, R.-E., Knopf, D. A., Veselovskii, I., Baars, H., Engelmann, R., Foth, A., Jimenez, C., Seifert, P., and Barja, B.: Tropospheric and stratospheric wildfire smoke profiling with lidar: mass, surface area, CCN, and INP retrieval, Atmos. Chem. Phys., 21, 9779–9807, https://doi.org/10.5194/acp-21-9779-2021, 2021.

Apituley, Arnoud, Mattia Pedergnana, Maarten Sneep, J. Pepijn Veefkind, Diego Loyola, Bram Sanders, Martin de Graaf, Sentinel-5 precursor/TROPOMI Level 2 Product User Manual Aerosol Layer Height, S5P-KNMI-L2-0022-MA, issue 2.0.1, 2021-11-15, CI-7570-PUM, https://sentinels.copernicus.eu/documents/247904/2474726/Sentinel-5P-Level-2-Product-User-Manual-Aerosol-Layer-Height, last access: 14.12.2021, 2021.

Baars, H., Ansmann, A., Engelmann, R., and Althausen, D.: Continuous monitoring of the boundary-layer top with lidar, Atmos. Chem. Phys., 8, 7281–7296, https://doi.org/10.5194/acp-8-7281-2008, 2008.

Baars, H., Kanitz, T., Engelmann, R., Althausen, D., Heese, B., Komppula, M., Preißler, J., Tesche, M., Ansmann, A.,Wandinger, U., Lim, J.-H., Ahn, J. Y., Stachlewska, I. S.,Amiridis, V., Marinou, E., Seifert, P., Hofer, J., Skupin, A.,Schneider, F., Bohlmann, S., Foth, A., Bley, S., Pfüller, A., Giannakaki, E., Lihavainen, H., Viisanen, Y., Hooda, R. K., Pereira, S. N., Bortoli, D., Wagner, F., Mattis, I., Janicka, L., Markowicz, K. M., Achtert, P., Artaxo, P., Pauliquevis, T., Souza, R. A. F.,Sharma, V. P., van Zyl, P. G., Beukes, J. P., Sun, J., Rohwer, E.G., Deng, R., Mamouri, R.-E., and Zamorano, F.: An overview of the first decade of PollyNET: an emerging network of automated Raman-polarization lidars for continuous aerosol profiling, Atmos. Chem. Phys., 16, 5111–5137, doi:10.5194/acp-16-5111-2016, 2016

Baars, H., Radenz, M., Floutsi, A. A., Engelmann, R., Althausen, D., Heese, B., Ansmann, A., Flament, T., Dabas, A., Trapon, D., Reitebuch, O., Bley, S., and Wandinger, U.: Californian Wildfire Smoke Over Europe: A First Example of the Aerosol Observing Capabilities of Aeolus Compared to Ground-Based Lidar, Geophys. Res. Lett., 48, e2020GL092194, https://doi.org/10.1029/2020GL092194, 2021

Balis, D., Giannakaki, E., Müller, D., Amiridis, V., Kelektsoglou, K., Rapsomanikis, S., and Bais, A.: Estimation of the microphysical aerosol properties over Thessaloniki, Greece, during the SCOUT-O3 campaign with the synergy of Raman lidar and sunphotometer data, J. Geophys. Res., 115, D08202, https://doi.org/10.1029/2009JD013088, 2010.

Basart, S., C. Pérez, E. Cuevas, J.M. Baldasano, and G.P. Gobbi, 2009: Aerosol characterization in Northern Africa, Northeastern Atlantic, Mediterranean Basin and Middle East from direct-sun AERONET observations. *Atmos. Chem. Phys.*, 9, 8265-8282, doi:10.5194/acp-9-8265-2009.

Chen Xi, Wang Jun , Xu Xiaoguang, Zhou Meng , Zhang Huanxin , Castro Garcia Lorena, Colarco Peter R., Janz Scott J., Yorks John, McGill Matthew, Reid S. Jeffrey, de Graaf Martin, Kondragunta Shobha.: First retrieval of absorbing aerosol height over dark target using TROPOMI oxygen B band: Algorithm development and application for surface particulate matter estimates, Remote Sensing of Environment, Volume 265, 2021, 112674, ISSN 0034-4257, https://doi.org/10.1016/j.rse.2021.112674, 2021.

Chiapello, I., Formenti, P., Mbemba Kabuiku, L., Ducos, F., Tanré, D., and Dulac, F.: Aerosol optical properties derived from POLDER-3/PARASOL (2005–2013) over the Western Mediterranean Sea – Part 2: Spatial distribution and temporal variability, Atmos. Chem. Phys., 21, 12715–12737, https://doi.org/10.5194/acp-21-12715-2021, 2021.

D'Amico, G., Amodeo, A., Baars, H., Binietoglou, I., Freudenthaler, V., Mattis, I., Wandinger, U., and Pappalardo, G.: EARLINET Single Calculus Chain – overview on methodology and strategy, Atmos. Meas. Tech., 8, 4891–4916, https://doi.org/10.5194/amt-8-4891-2015, 2015.

D'Amico, G., Amodeo, A., Mattis, I., Freudenthaler, V., and Pappalardo, G.: EARLINET Single Calculus Chain – technical – Part 1: Pre-processing of raw lidar data, Atmos. Meas. Tech., 9, 491–507, https://doi.org/10.5194/amt-9-491-2016, 2016.

https://doi.org/10.5194/acp-2022-412
Preprint. Discussion started: 18 July 2022

Atmospheric Chemistry and Physics Discussions

de Graaf, M., J.F. de Haan and A.F.J. Sanders, TROPOMI ATBD Aerosol Layer Height, issue 2.2.0, 2021-07-05, S5P-KNMI-L2-0006-RP, CI-7430-ATBD_Aerosol_Layer_Height, https://sentinels.copernicus.eu/documents/247904/2476257/Sentinel-5P-TROPOMI-ATBD-Aerosol-Height, (last access: 01.05.2022), 2021.

de Graaf, M., Stammes, P., Torres, O., and Koelemeijer, R. B.: Absorbing Aerosol Index: Sensitivity analysis, application to GOME and comparison with TOMS, J. Geophys. Res.-Atmos. 110, 1–19, https://doi.org/10.1029/2004JD005178, 2005.

Engelmann, R., Kanitz, T., Baars, H., Heese, B., Althausen, D., Skupin, A., Wandinger, U., Komppula, M., Stachlewska, I. S., Amiridis, V., Marinou, E., Mattis, I., Linné, H., and Ansmann, A.: The automated multiwavelength Raman polarization and water-vapor lidar PollyXT: the neXT generation, Atmos. Meas. Tech., 9, 1767–1784, https://doi.org/10.5194/amt-9-1767-2016, 2016

Georgoulias, A. K., Marinou, E., Tsekeri, A., Proestakis, E., Akritidis, D., Alexandri, G., Zanis, P., Balis, D., Marenco, F., Tesche, M. and Amiridis, V.: A first case study of CCN concentrations from Spaceborne Lidar Observations, Remote Sens. 2020, 12(10), 1557, https://doi.org/10.3390/rs12101557, 2020.

Gerasopoulos, E., Amiridis, V., Kazadzis, S., Kokkalis, P., Eleftheratos, K., Andreae, M. O., Andreae, T. W., El-Askary, H., and Zerefos, C. S.: Three-year ground based measurements of aerosol optical depth over the Eastern Mediterranean: the urban environment of Athens, Atmos. Chem. Phys., 11, 2145–2159, https://doi.org/10.5194/acp-11-2145-2011, 2011.

Granados-Muñoz, M. J., Bravo-Aranda, J. A., Baumgardner, D., Guerrero-Rascado, J. L., Pérez-Ramírez, D., Navas-Guzmán, F., Veselovskii, I., Lyamani, H., Valenzuela, A., Olmo, F. J., Titos, G., Andrey, J., Chaikovsky, A., Dubovik, O., Gil-Ojeda, M., and Alados-Arboledas, L.: A comparative study of aerosol microphysical properties retrieved from ground-based remote sensing and aircraft in situ measurements during a Saharan dust event, Atmos. Meas. Tech., 9, 1113–1133, https://doi.org/10.5194/amt-9-1113-2016, 2016.

Griffin, D., Sioris, C., Chen, J., Dickson, N., Kovachik, A., de Graaf, M., Nanda, S., Veefkind, P., Dammers, E., McLinden, C. A., Makar, P., and Akingunola, A.: The 2018 fire season in North America as seen by TROPOMI: aerosol layer height intercomparisons and evaluation of model-derived plume heights, Atmos. Meas. Tech., 13, 1427–1445, https://doi.org/10.5194/amt-13-1427-2020, 2020.

Hassinen, S., Balis, D., Bauer, H., Begoin, M., Delcloo, A., Eleftheratos, K., Gimeno Garcia, S., Granville, J., Grossi, M., Hao, N., Hedelt, P., Hendrick, F., Hess, M., Heue, K.-P., Hovila, J., Jønch-Sørensen, H., Kalakoski, N., Kauppi, A., Kiemle, S., Kins, L., Koukouli, M. E., Kujanpää, J., Lambert, J.-C., Lang, R., Lerot, C., Loyola, D., Pedergnana, M., Pinardi, G., Romahn, F., van Roozendael, M., Lutz, R., De Smedt, I., Stammes, P., Steinbrecht, W., Tamminen, J., Theys, N., Tilstra, L. G., Tuinder, O. N. E., Valks, P., Zerefos, C., Zimmer, W., and Zyrichidou, I.: Overview of the O3M SAF GOME-2 operational atmospheric composition and UV radiation data products and data availability, Atmos. Meas. Tech., 9, 383–407, https://doi.org/10.5194/amt-9-383-2016, 2016.

Ingmann, P., Veihelmann, B., Langen, J., Lamarre, D., Stark, H., and Courrèges-Lacoste, G. B.: Requirements for the GMES Atmosphere Service and ESA's implementation concept: Sentinels-4/-5 and -5p, Remote Sens. Environ., 120, 58–69, https://doi.org/10.1016/j.rse.2012.01.023, 2012.

IPCC, 2021: Climate Change 2021: The Physical Science Basis. Contribution of Working Group I to the Sixth Assessment Report of the Intergovernmental Panel on Climate Change [Masson-Delmotte, V., P. Zhai, A. Pirani, S.L. Connors, C. Péan, S. Berger, N. Caud, Y. Chen, L. Goldfarb, M.I. Gomis, M. Huang, K. Leitzell, E. Lonnoy, J.B.R. Matthews, T.K. Maycock, T. Waterfield, O. Yelekçi, R. Yu,and B. Zhou (eds.)]. Cambridge University Press. In Press.

Kampouri, A., Amiridis, V., Solomos, S., Gialitaki, A., Marinou, E., Spyrou, C., Georgoulias, A.K., Akritidis, D., Papagiannopoulos, N., Mona, L., Scollo, S., Tsichla, M., Tsikoudi, I., Pytharoulis, I., Karacostas, T., and Zanis, P.: Investigation of Volcanic Emissions in the Mediterranean: "The Etna–Antikythera Connection", Atmosphere 2021, 12(1), 40; https://doi.org/10.3390/atmos12010040, 2021.

Klett, J. D.: Stable analytical inversion solution for processing lidar returns, Appl. Optics, 20, 211–220, 1981.

https://doi.org/10.5194/acp-2022-412
Preprint. Discussion started: 18 July 2022

Kim, J., Jeong, U., Ahn, M.-H., Kim, J. H., Park, R. J., Lee, H., Song, C. H., Choi, Y.-S., Lee, K.-H., Yoo, J.-M., Jeong, M.-J., Park, S. K., Lee, K.-M., Song, C.-K., Kim, S.-W., Kim, Y. J., Kim, S.-W., Kim, M., Go, S., Liu, X., Chance, K., Chan Miller, C., Al-Saadi, J., Veihelmann, B., Bhartia, P. K., Torres, O., Abad, G. G., Haffner, D. P., Ko, D. H., Lee, S. H., Woo, J.-H., Chong, H., Park, S. S., Nicks, D., Choi, W. J., Moon, K.-J., Cho, A., Yoon, J., Kim, S.-K., Hong, H., Lee, K., Lee, H., Lee, S., Choi, M., Veefkind, P., Levelt, P. F., Edwards, D. P., Kang, M., Eo, M., Bak, J., Baek, K., Kwon, H.-A., Yang, J., Park, J., Han, K. M., Kim, B.-R., Shin, H.-W., Choi, H., Lee, E., Chong, J., Cha, Y., Koo, J.-H., Irie, H., Hayashida, S., Kasai, Y., Kanaya, Y., Liu, C., Lin, J., Crawford, J. H., Carmichael, G. R., Newchurch, M. J., Lefer, B. L., Herman, J. R., Swap, R. J., Lau, A. K. H., Kurosu, T. P., Jaross, G., Ahlers, B., Dobber, M., McElroy, C. T., and Choi, Y.: New Era of Air Quality Monitoring from Space: Geostationary Environment Monitoring Spectrometer (GEMS), B. Am. Meteorol. Soc., 101, E1–E22, https://doi.org/10.1175/BAMS-D-18-0013.1, 2019.

Lelieveld J, Berresheim H, Borrmann S, Crutzen PJ, Dentener FJ, Fischer H, Feichter J, Flatau PJ, Heland J, Holzinger R, Korrmann R, Lawrence MG, Levin Z, Markowicz KM, Mihalopoulos N, Minikin A, Ramanathan V, De Reus M, Roelofs GJ, Scheeren HA, Sciare J, Schlager H, Schultz M, Siegmund P, Steil B, Stephanou EG, Stier P, Traub M, Warneke C, Williams J, Ziereis H. Global air pollution crossroads over the Mediterranean. Science. 2002 Oct 25; 298(5594):794-9. doi: 10.1126/science.1075457. PMID: 12399583.

Mallet, M., Dubovik, O., Nabat, P., Dulac, F., Kahn, R., Sciare, J., Paronis, D., and Léon, J. F.: Absorption properties of Mediterranean aerosols obtained from multi-year ground-based remote sensing observations, Atmos. Chem. Phys., 13, 9195–9210, https://doi.org/10.5194/acp-13-9195-2013, 2013.

Marinou, E., Amiridis, V., Binietoglou, I., Tsikerdekis, A., Solomos, S., Proestakis, E., Konsta, D., Papagiannopoulos, N., Tsekeri, A., Vlastou, G., Zanis, P., Balis, D., Wandinger, U., and Ansmann, A.: Three-dimensional evolution of Saharan dust transport towards Europe based on a 9-year EARLINET-optimized CALIPSO dataset, Atmos. Chem. Phys., 17, 5893–5919, https://doi.org/10.5194/acp-17-5893-2017, 2017.

Michailidis, K., Koukouli, M.-E., Siomos, N., Balis, D., Tuinder, O., Tilstra, L. G., Mona, L., Pappalardo, G., and Bortoli, D.: First validation of GOME-2/MetOp absorbing aerosol height using EARLINET lidar observations, Atmos. Chem. Phys., 21, 3193–3213, https://doi.org/10.5194/acp-21-3193-2021, 2021.

Mona, L., Amodeo, A., Pandolfi, M., and Pappalardo, G.: Saharan dust intrusions in the Mediterranean area: three years of Raman lidar measurements, J. Geophys. Res.-Atmos., 111, d16203, doi:10.1029/2005JD006569, 2006.

Mona, L., Liu, Z., Müller, D., Omar, A., Papayannis, A., Pappalardo, G., Sugimoto, N., and Vaughan, M.: Lidar measurements for desert dust characterization: An overview, Adv. Meteorol., 2012, 36 pp., https://doi.org/10.1155/2012/356265, 2012.

Nabat, P., Somot, S., Mallet, M., Chiapello, I., Morcrette, J. J., Solmon, F., Szopa, S., Dulac, F., Collins, W., Ghan, S., Horowitz, L. W., Lamarque, J. F., Lee, Y. H., Naik, V., Nagashima, T., Shindell, D., and Skeie, R.: A 4-D climatology (1979–2009) of the monthly tropospheric aerosol optical depth distribution over the Mediterranean region from a comparative evaluation and blending of remote sensing and model products, Atmos. Meas. Tech., 6, 1287–1314, https://doi.org/10.5194/amt-6-1287-2013, 2013.

Nanda, S., de Graaf, M., Veefkind, J. P., Sneep, M., ter Linden, M., Sun, J., and Levelt, P. F.: A first comparison of TROPOMI aerosol layer height (ALH) to CALIOP data, Atmos. Meas. Tech., 13, 3043–3059, https://doi.org/10.5194/amt-13-3043-2020, 2020.

Nanda, S., de Graaf, M., Veefkind, J. P., ter Linden, M., Sneep, M., de Haan, J., and Levelt, P. F.: A neural network radiative transfer model approach applied to the Tropospheric Monitoring Instrument aerosol height algorithm, Atmos. Meas. Tech., 12, 6619–6634, https://doi.org/10.5194/amt-12-6619-2019, 2019.

Obregón, M.A.; Costa, M. J.; Silva, A.M.: Serrano, A.: Spatial and Temporal Variation of Aerosol and Water Vapour Effects on Solar Radiation in the Mediterranean Basin during the Last Two Decades. Remote Sens., 12, 1316, https://doi.org/10.3390/rs12081316, 2020.

https://doi.org/10.5194/acp-2022-412
Preprint. Discussion started: 18 July 2022

Nelson, D. L., Garay, M. J., Kahn, R. A., and Dunst, B. A.: Stereoscopic height and wind retrievals for aerosol plumes with the MISR INteractive eXplorer (MINX), Remote Sens.-Basel, 5, 4593–4628, https://doi.org/10.3390/rs5094593, 2013.

Ortiz-Amezcua, P., Guerrero-Rascado, J. L., Granados-Muñoz, M. J., Benavent-Oltra, J. A., Böckmann, C., Samaras, S., Stachlewska, I. S., Janicka, Ł., Baars, H., Bohlmann, S., and Alados-Arboledas, L.: Microphysical characterization of long-range transported biomass burning particles from North America at three EARLINET stations, Atmos. Chem. Phys., 17, 5931–5946, https://doi.org/10.5194/acp-17-5931-2017, 2017

Papagiannopoulos, N., Mona, L., Alados-Arboledas, L., Amiridis, V., Baars, H., Binietoglou, I., Bortoli, D., D'Amico, G., Giunta, A., Guerrero-Rascado, J. L., Schwarz, A., Pereira, S., Spinelli, N., Wandinger, U., Wang, X., and Pappalardo, G.: CALIPSO climatological products: evaluation and suggestions from EARLINET, Atmos. Chem. Phys., 16, 2341–2357, https://doi.org/10.5194/acp-16-2341-2016, 2016.

Papagiannopoulos, N., Mona, L., Amodeo, A., D'Amico, G., Gumà Claramunt, P., Pappalardo, G., Alados-Arboledas, L., Guerrero-Rascado, J.L., Amiridis, V., Apituley, A., Baars, H., Scwharz, A., Wandinger, U., Binietoglou, I., Nicolae, D., Bortoli, D., Kokkalis, P., Papayannis, A., Rodriguez-Gómez, A., Sicard, M., Wiegner M., Comerón, A.: An automatic observation-based typing method for EARLINET, Atmos. Chem. Phys.,18, 15879-15901, 2018.

Papanikolaou, C.A,, Giannakaki, E., Papayannis, A., Mylonaki, M., Soupiona, O.: Canadian biomass burning aerosol properties modification during a long-ranged event on August 2018, *Sensors*, 20, 5442; doi:10.3390/s20185442, 2020.

Romano, S., Burlizzi, P., Kinne, S., De Tomasi, F., Hamann, U., Perrone, M.R., 2018. Radiative impact of Etna volcanic aerosols over south eastern Italy on 3 December 2015. Atmos. Environ. 182, 155-170. DOI: 10.1016/j.atmosenv.2018.03.038.

Papayannis, A., Amiridis, V., Mona, L., Tsaknakis,G., Balis, D., Bösenberg, J., Chaikovski, A., Tomasi, F. De., Grigorov, I., Mattis, I., Mitev, V., Müller, D., Nickovic, S., Pérez, C., Pietruczuk, A., Pisani, L., Ravetta, F., Rizi, V., Sicard, M., Trickl, T., Wiegner, M., Gerding, M., Mamouri, R. E., D'Amico, G., Pappalardo, G.: Systematic lidar observations of Saharan dust over Europe in the frame of EARLINET (2000-2002), J. Geophys. Res.,113, D10204, doi:10.1029/2007JD009028, 2008.

Pappalardo, G., Amodeo, A., Apituley, A., Comeron, A., Freudenthaler, V., Linné, H., Ansmann, A., Bösenberg, J., D'Amico, G., Mattis, I., Mona, L., Wandinger, U., Amiridis, V., Alados-Arboledas, L., Nicolae, D., and Wiegner, M.: EARLINET: towards an advanced sustainable European aerosol lidar network, Atmos. Meas. Tech., 7, 2389–2409, https://doi.org/10.5194/amt-7-2389-2014, 2014

Perrone, M.R. and Romano, S.: Atmospheric response to the 20 March 2015 solar eclipse along the whole aerosol column by lidar measurements. Atmospheric Research, Volume 217, 2019, Pages 172-183, https://doi.org/10.1016/j.atmosres.2018.11.004, 2019

Proestakis, E., Amiridis, V., Marinou, E., Binietoglou, I., Ansmann, A., Wandinger, U., Hofer, J., Yorks, J., Nowottnick, E., Makhmudov, A., Papayannis, A., Pietruczuk, A., Gialitaki, A., Apituley, A., Szkop, A., Muñoz Porcar, C., Bortoli, D., Dionisi, D., Althausen, D., Mamali, D., Balis, D., Nicolae, D., Tetoni, E., Liberti, G. L., Baars, H., Mattis, I., Stachlewska, I. S., Voudouri, K. A., Mona, L., Mylonaki, M., Perrone, M. R., Costa, M. J., Sicard, M., Papagiannopoulos, N., Siomos, N., Burlizzi, P., Pauly, R., Engelmann, R., Abdullaev, S., and Pappalardo, G.: EARLINET evaluation of the CATS Level 2 aerosol backscatter coefficient product, Atmos. Chem. Phys., 19, 11743–11764, https://doi.org/10.5194/acp-19-11743-2019, 2019.

Salgueiro, V., Costa, M. J., Guerrero-Rascado, J. L., Couto, F. T., and D. Bortoli, 2021: Characterization of forest fire and Saharan desert dust aerosols over South-western Europe using a multi-wavelength Raman lidar and Sun-photometer. Atmospheric Environment, 118346, https://doi.org/10.1016/j.atmosenv.2021.118346, 2021.

https://doi.org/10.5194/acp-2022-412
Preprint. Discussion started: 18 July 2022

Sanders, A. F. J., de Haan, J. F., Sneep, M., Apituley, A., Stammes, P., Vieitez, M. O., Tilstra, L. G., Tuinder, O. N. E., Koning, C. E., and Veefkind, J. P.: Evaluation of the operational Aerosol Layer Height retrieval algorithm for Sentinel-5 Precursor: application to O2 A band observations from GOME-2A, Atmos. Meas. Tech., 8, 4947–4977, https://doi.org/10.5194/amt-8-4947-2015, 2015.

Siomos, N., Balis, D. S., Voudouri, K. A., Giannakaki, E., Filioglou, M., Amiridis, V., Papayannis, A., and Fragkos, K.: Are EARLINET and AERONET climatologies consistent? The case of Thessaloniki, Greece, Atmos. Chem. Phys., 18, 11885–11903, https://doi.org/10.5194/acp-18-11885-2018, 2018.

Soupiona, O., Papayannis, A., Kokkalis, P., Foskinis, R., Sánchez Hernández, G., Ortiz-Amezcua, P., Mylonaki, M., Papanikolaou, C.-A., Papagiannopoulos, N., Samaras, S., Groß, S., Mamouri, R.-E., Alados-Arboledas, L., Amodeo, A., and Psiloglou, B.: EARLINET observations of Saharan dust intrusions over the northern Mediterranean region (2014–2017): properties and impact on radiative forcing, Atmos. Chem. Phys., 20, 15147–15166, https://doi.org/10.5194/acp-20-15147-2020, 2020.

Stein Zweers, D. C.: TROPOMI ATBD of the UV aerosol index, S5P-KNMI-L2-0008-RP, CI-7430-ATBD_UVAI, issue 2.0, 2021-07-05, https://sentinels.copernicus.eu/documents/247904/2476257/Sentinel-5P-TROPOMI-ATBD-UV-Aerosol-Index, last access: 01.05.2022, 2021.

Stein, A. F., Draxler, R. R., Rolph, G. D., Stunder, B. J. B., Cohen, M. D., and Ngan, F.: NOAA's hysplit atmospheric transport and dispersion modeling system, B. Am. Meteorol. Soc., 96, 2059–2077, https://doi.org/10.1175/BAMS-D-14-00110.1, 2015

Torres, O., Bhartia, P. K., Herman, J. R., Ahmad, Z., and Gleason, J.: Derivation of aerosol properties from satellite measurements of backscattered ultraviolet radiation: Theoretical basis, J. Geophys. Res.-Atmos., 103, 17099–17110, https://doi.org/10.1029/98JD00900, 1998.

Winker, D. M., Vaughan, M. A., Omar, A., Hu, Y., Powell, K. A., Liu, Z., Hunt, W. H., and Young, S. A.: Overview of the CALIPSO mission and CALIOP data processing algorithms, J. Atmos. Ocean. Technol., 26, 2310–2323, https://doi.org/10.1175/2009JTECHA1281.1, 2009.

Xu, X., Wang, J., Wang, Y., Zeng, J., Torres, O., Reid, J. S.,Miller, S. D., Martins, J. V., and Remer, L. A.: Detecting layer height of smoke aerosols over vegetated land and water surfaces via oxygen absorption bands: hourly results from EPIC/DSCOVR in deep space, Atmos. Meas. Tech., 12, 3269–3288, https://doi.org/10.5194/amt-12-3269-2019, 2019.

https://doi.org/10.5194/acp-2022-412
Preprint. Discussion started: 18 July 2022

Appendix A1: Validation methodology flowchart

Figure A 1 shows a synoptic flowchart of the data processing according to validation methodology following in this study.

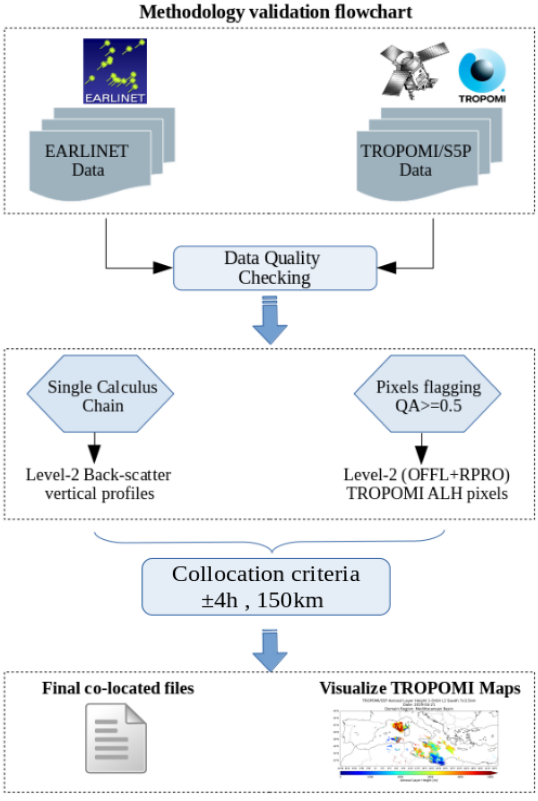

Figure A 1. Flowchart of the validation approach.

Appendix A2. Aerosol layering using WCT method

This section aims at illustrating how the Wavelet covariance Transform method can be used on LIDAR backscatter profiles for layer detection. We use the wavelet covariance transform following the scheme proposed by Michailidis et al. (2021). The aerosol geometrical properties carry information about the structure of lidar profiles, such as the boundary layer height and the features of the lofted aerosol layers and can be obtained from any lidar profile. Some lidar optical products, however, are more reliable to use than others. For example, the longer wavelengths typically magnify the differences in the vertical distribution of the aerosol load, resulting in layers that are easier to identify. This is the reason why we prioritize them so as to produce geometrical properties. The product with the highest potential to magnify the aerosol layer structure available is selected for each measurement. A critical parameter for the accurate WCT application is the selection of an appropriate value

https://doi.org/10.5194/acp-2022-412
Preprint. Discussion started: 18 July 2022

Atmospheric Chemistry and Physics Discussions

for the window (dilation), to distinguish cloud layers from aerosol layers. In our case, a dilation of 0.5 km is used for the selected backscatter profiles according to Baars et al. (2008). Then, the algorithm scans the profile, searching for pairs of boundaries (base-top). Details about the WCT method can be found in Siomos et al. (2018) and Michailidis et al. (2021). An example of a lidar backscatter profile with resulting WCT profile from the Antikythera (PANGEA-NOA) lidar station 27 May 2019 is given in . This figure reasonably shows the ability of the lidar to detect multiple layers. The horizontal dashed blue and red lines represent the detected aerosol layer base and top applying the WCT methodology, and two aerosol layers are detected, according the methodology that we follow.

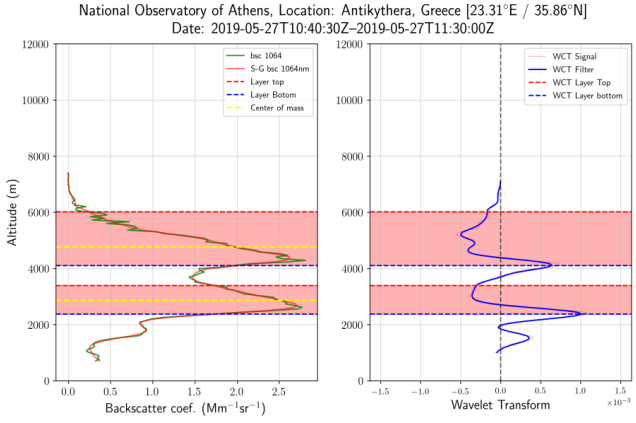

Figure A 2. Antikythera PollyXT lidar (PANGEA- NOA): (a) lidar backscatter profile at 532 nm and (b) resulting WCT profile on 27 May 2019. The horizontal dashed red and blue lines represent the detected aerosol layer top and base applying the WCT methodology. The label "S–G" indicates that a Savitzky–Golay filter was used to signal smoothing. The yellow horizontal line represent the center of mass for each detected layer.